

SLAC-PUB-2025
October 1977
(T/E)

THE EXPERIMENTAL BASIS FOR THE NEW QUARK SPECTROSCOPY*

by

W. K. H. Panofsky

Stanford Linear Accelerator Center

Stanford, California 95305

*CENTENNIAL MEETING
MATHEMATICAL AND PHYSICAL SOCIETIES OF JAPAN,
TOKYO, OCTOBER 10, 1977*

This paper is the content of a talk at the Centennial Meeting of the Mathematical and Physical Societies of Japan on October 10, 1977 in Tokyo. It represents a survey to be delivered to an audience of physicists working in a variety of fields covering the recent developments in high-energy particle spectroscopy. The work covers contributions from many laboratories in the U.S. and abroad, and there was no way to give credit to individual contributions. I would like to acknowledge my gratitude to the many authors and their institutions and I would like to apologize for any errors or omissions in covering their work.

*Work supported by the Department of Energy

I. INTRODUCTION

The events in high-energy physics that occurred in November 1974 have justly been described as a revolution. The specific phenomena discovered at that time had not been predicted by anyone, although the basic structures which were unveiled did reinforce certain ideas that pointed toward an expansion of the family of quarks and leptons, which had been anticipated by some. These discoveries were followed by a period of unprecedented productivity in particle physics that has lent increased credibility to the concept that quarks are indeed the constituents of hadrons, and that quarks together with leptons might fulfill the condition of "elementarity"- that is, that these particles would not reveal any internal structure. Yet this elementarity is in itself a paradox. It says that what we actually observe in nature is simply the debris from complex interactions and from violations of the inherent symmetry of the elementary framework.

Our present theoretical understanding, or lack of understanding, of this paradoxical situation will be discussed by other speakers at this meeting, who will also tell us that the recent proliferation of apparently elementary building blocks in nature appears to be a likely guide to ultimately unifying concepts. My task here will be to review the experimental basis of the recent findings in order to give you a calibration of the reliability of the foundations upon which this theoretical understanding has been built.

II. THE SITUATION PRIOR TO NOVEMBER 1974

Beginning with the discoveries of particle resonances at Berkeley and of strange particles in the cosmic radiation, there commenced a veritable explosion of new particles and particle states. This led the late Professor Oppenheimer to make his much-quoted statement that discovery of a new particle, rather than being rewarded by a Nobel Prize, should receive a \$10,000 fine. Gell-Mann and Zweig brought order into this chaos by introducing the concept of three quarks being fundamental building blocks which in various combinations constitute the families of particles as actually observed. This conjecture

not only explained the profusion of particles and resonant states that the experimentalists had uncovered but also had predictive value for discovery of new objects and correction of past errors.

Many theorists in many parts of the world, including the originators of the original three quark proposal, emphasized that the group of three quarks could be broadened to a four quark scheme. In fact it was emphasized that such an arrangement would exhibit an attractive symmetry with the four leptons, consisting of the two doublets of electrons and muons with their respective neutrinos.

However, it was specific theoretical arguments and experimental evidence which led to an increased conviction that the simple three quark picture not only permitted, but required, augmentation.

The first difficulty of the simple three quark model related to the structure of the nucleon (i.e., the neutron and proton), which was believed to be composed of three quarks, each of spin $1/2$, but in a symmetric ground state. To rectify this violation of the relation of spin and statistics, it was proposed that quarks could exhibit three "colors" as additional quantum numbers, but that objects observable in nature would always be color singlets, that is, have a net quantum number of color equal to zero. Then there was also the observation that apparently weak decays involving change in strangeness but not change in charge appeared to be inhibited, as was manifested in particular by the anomalously small decay rate of the neutral kaon into two muons. This phenomenon, could be explained by the inclusion of a fourth quark which permitted the introduction of additional selection rules. Figure 1 lists the quarks and their basic characteristics corresponding to this 4-quark picture.

The idea that nucleons contain point-like or almost point-like building blocks was given increased credence through the experiments on deep inelastic electron scattering. Here it was observed in the early days of the SLAC

accelerator that the number of inelastic electron scattering events on protons and neutrons involving large momentum transfer greatly exceeded the number expected if these nucleons were composed of continuous matter distributed within a radius determined previously by elastic electron scattering and nuclear observations. Rather, the angular and energy distribution of inelastically scattered electrons exhibited surprising agreement with those kinematic conditions which would be expected if scattering took place on point-like subunits, then dubbed "partons" which would be present in the nucleons. It is now presumed that the partons and quarks are identical objects.

III. DISCOVERY OF THE ψ/J

This is where matters stood in November 1974. At that time, as is now well known, Sam Ting and collaborators at Brookhaven, and Burt Richter and collaborators at SLAC published simultaneously the sharp peak in the effective mass spectrum of electron-positron pairs formed by nucleon-nucleon collisions, and the even sharper peak in the energy dependence of the production of hadrons by electron-positron annihilation, respectively. These peaks are shown in Figures 2 and 3. These discoveries sent a shock through the scientific community. Specifically, they demonstrated beyond a reasonable doubt that there had to exist additional quantum numbers and selection rules to account for the narrowness of the states in question. Many theoretical speculations followed. I will not discuss these here, but I will assume in the discussion to follow that the new quantum number is identified with the fourth quark proposed earlier by many theorists and named "charm" by Bjorken and Glashow. It is now well established that the particle discovered in these experiments, called the J or ψ by their respective authors, is a bound state of the charmed quark and its antiparticle - that is, the object dubbed "charmonium" of net charm quantum number zero. This explanation received additional credence by the discovery, shortly thereafter, of a second narrow resonance called the ψ' , that was interpreted as the first radially excited state of the ψ/J .

The width of the ψ/J and ψ' can be determined absolutely by reference to the diagrams shown in Figure 4, which shows their production and subsequent decay either into hadrons or into electron pairs. Note that in the former diagram the vertex between the electron pair, and the ψ/J , or the ψ' , occurs only once, while in the diagram governing the decay of the ψ/J or the ψ' into electrons the same vertex appears twice. Accordingly, comparison of the cross-sections permits an absolute determination of the width by the formula

$$\Gamma_{e^+e^-} = \left(m^2 / 6\pi^2 \right) \int \sigma_{\text{total}} dE$$

which leads to an absolute total width of magnitude 69 ± 15 KeV for the ψ/J of mass 3095 ± 4 MeV, and to 228 ± 56 KeV for the ψ' of mass 3684 ± 5 MeV.

This width is, of course, much smaller than the experimental resolution of the two experiments in which the ψ/J was originally discovered. In the Brookhaven experiment, which measured the effective mass of electron pairs, the observed width is governed by the resolution of the double-armed spectrometer used. This spectrometer is shown in Figure 5. In the SLAC experiment, the resolution is governed by the energy spread of the colliding electron and positron beams in the SPEAR storage ring. The SPEAR ring is shown in Figure 6. The energy resolution of SPEAR's beams depends on the equilibrium that is established between the excitation of the spread in energy driven by quantum fluctuations of the emitted synchrotron radiation and the damping of such oscillations through radiation. The resulting energy width is about 1 MeV, which is broader than the calculated resonance widths.

In this talk I can touch only briefly on the experimental apparatus that was used in making the original discoveries, and from which the subsequent flood of important information has come. The largest part of this data has come from electron-positron annihilation, although the new particles have also been produced in stationary-target experiments using beams of photons,

protons, neutrons, kaons and pions. The most productive means for observing the products of e^+e^- annihilation has been to surround the interaction region with a detector that has as large a solid angle as possible, that can measure with reasonable accuracy the momenta of charged particles, and that also has some capabilities in particle identification. It has also become clear that neutral-particle detection is increasingly important. Figure 7 shows the Mark I magnetic detector with which the original discoveries were made at the SPEAR storage ring at SLAC, and which has been the main work horse for the subsequent experiments at SPEAR. Events detected in the Mark I are logged into an associated computer, and several typical events as reconstructed by the computer are shown in the next three figures. Figure 8 shows either elastic e^+e^- scattering, or annihilation into just a single charged-particle pair, both leading to collinearity of the detected pair. Figure 9 shows a hadron-production event in which only two charged tracks are visible. Figure 10 shows more complex hadron-production events.

If we assume that the ψ/J is indeed a bound state of charmed quarks, then its width can be understood by analogy with the observed width of the ϕ meson, which is known to be a bound state of the strange quark with its antiparticle. As shown in Figure 11, the width is determined by what is known as the OZI (Okubo-Zweig-Iizuka) rule, which states that any reaction in which a quark line bends back on to itself (i.e., in which a quark-antiquark pair internally annihilates or is created) will be forbidden by a substantial factor. As is seen from the diagram, the decay of the ϕ meson into three pions would thus be forbidden, while decay into two K mesons is allowed but is inhibited by the limited phase space resulting from the small mass difference involved. In the analogous case of the psions (we will call the ψ/J , ψ' , etc. "psions"), a decay into two "charmed particles" - that is, into two particles each of net charm quantum number different from zero - would be allowed, but, as we shall see later, is energetically impossible. Accordingly, decay of the ψ/J and ψ' can proceed only through processes that are totally forbidden by the OZI rule.

IV. THE EVIDENCE FOR CHARMONIUM

Let us now examine the evidence on which the conclusion rests that the psions are bound states of charmonium, and let us also examine the basis for quantum number assignments to these objects. We conclude first that these particles have the same quantum numbers as the photon. It has been observed, as is shown in Figure 12, that the amplitude for the production and subsequent decay of these particles into lepton pairs interferes with the direct electromagnetic production of lepton pairs by e^+e^- annihilation. This interference is demonstrated by the observed distortion of the resonant peaks. Therefore the psions and the photon each have spin 1 and negative intrinsic parity. The vector character of the psions is also consistent with the photoproduction data from SLAC, Fermilab and Cornell, as shown in Figure 13. A number of features of these photoproduction data are of interest: First, the threshold of production appears to occur above the simple kinematic limit, indicating that at threshold these particles are not produced directly but by combination of a pair of intermediate objects. The observed threshold energy coincides with that required to produce charmed particles in pairs, that is, particles which are combinations of ordinary and charmed quarks, which then can combine into psions without violating the OZI rule. At high energy, on the other hand, it appears as if the cross section approaches a constant value; this is consistent with diffractive photoproduction of vector particles according to the mechanism shown in Figure 14 in which the photon directly converts into the vector particle which then scatters off the nucleon. As a result, these observations provide an indirect measurement of the psion-nucleon cross section, which is found to be near 1 millibarn.

Assuming that the vector character of the psions is established, one would like to fix their remaining quantum numbers. This determination rests on observation of the various hadronic decay modes. Fortunately, since the cross section at the peak of the psions is so large, many hundred thousand psion events have been recorded, and the branching ratios

into many decay modes have been determined. These decay modes are shown in Figure 15 for the ψ and in Figure 16 for the ψ' . Specifically, the so-called G-parity can be determined by observing the frequencies with which the psions decay into the even and odd numbers of pions, for the following reason. At the resonance peaks, pions can be created either through direct psion decay or through the two-step process in which the psion is converted into a virtual photon which then creates the pions. This is illustrated in Figure 17. Since the latter process is electromagnetic, isotopic spin and G-parity are not conserved as they are in the strong interactions. However, from the substantial psion-nucleon cross section noted above we already know that the psions are in fact hadrons, and we thus expect these quantum numbers to be conserved when the psions decay directly into pions.

Decays of the psions into odd and even numbers of pions are shown in Figure 18, which clearly indicates that their G-parity must be odd. For a vector particle with G-parity odd the isotopic spin can be either 0 or 2. This question can be settled by observing psion decay into $p\bar{p}$ or $\Lambda\bar{\Lambda}$ pairs, and also by determining the ratios of psion decay into the various charge states of $\pi\rho$ combinations. The result of the observation of the nucleon-antinucleon pairs and of the $\pi\rho$ system leads to the definite conclusion that the J/ψ has isotopic spin zero.

The quantum numbers of the ψ' can be determined by a similar mechanism. The conclusion is that the quantum numbers of the ψ' and the J/ψ are the same. The principal basis of this conclusion is that the ψ' can decay into a combination of a J/ψ and an η which would be forbidden if the ψ' and J/ψ differed by two units in isotopic spin.

V. THE PSION FAMILY

From the above discussion we see that the psions represent a series of vector particles composed of quark pairs of a new quantum number, and having well-defined hadronic quantum numbers. Let us now inquire whether there are further members of this family; the answer is "yes." In Figures 19 and 20 we show the total hadronic production from electron-positron annihilation plotted as a function of energy of the annihilating particles.

The hadron yield is plotted as the ratio, R , of the cross section for hadron production to that for the production of muon pairs. In addition to the J/ψ and ψ' peaks (which are too large to be shown fully), there is a (recently discovered) peak at a center-of-mass energy of 3.77 GeV, followed by a complex region which appears to exhibit peaks at 4.03 GeV and 4.4 GeV, and perhaps also other possible structures. However, these higher peaks are definitely of broader width. Assuming that these peaks have the same intrinsic quantum numbers, the surmise is that they constitute radial excitations of the charm-anticharm quark combination. Qualitatively, this suggestion holds up under critical examination. However, quantitative attempts to fit the energies of these peaks with a simple potential model have not been fully successful.

The quantity R plotted in the previous figures is, as is well known, of the greatest intrinsic interest. If one believes that the process of hadron production from electron-positron annihilation proceeds via a single virtual photon, then the ratio of hadron production to the purely electromagnetic production of muon pairs is a direct measure of the square of the elementary charges into which the virtual photon can materialize. Figure 21 illustrates this assertion. In other words, the ratio R directly measures the sum of the squares of the elementary quark charges divided by the square of the electronic charge. If there were four quarks, half of which have charge $\pm 1/3$ and half of which have charge $\pm 2/3$, and if there were three colors of each of these quarks, then the ratio R should be $3-1/3$. Note that in Figure 19 R exhibits two plateaus: at energies below 3.5 GeV R has a value near 2, while at energies above 4.5 GeV it has a value above 4. These two plateaus are separated by the complex structures somehow related to charm. Apparently, therefore, the charm degree of freedom is being excited above a certain threshold, but the experimental data leave open the possibility that further objects may also exist beyond quarks of three "colors" and four "flavors."

The basic mechanism of electron-positron annihilation in the above description is assumed to be the creation of a pair of quarks by a virtual photon, followed by subsequent reactions involving the quark pair. The basic correctness of this description has been dramatically verified in the following way. If a virtual photon materializes into a quark pair, then this pair will be produced back-to-back along a certain axis (the so-called jet axis). As a result of this model, the angular distribution of the produced hadrons will not be isotropic but will tend to be aligned along the jet axis. This effect has been studied experimentally and found to be in excellent quantitative agreement with expectations. Specifically, as the energy grows, the deviation from the angular distribution predicted simply by phase space becomes increasingly pronounced, as shown in Figure 22. Moreover, the orientation of the jet axes relative to the direction of polarization of the electrons and positrons (the beams polarize naturally in an e^+e^- storage ring, albeit at a very slow pace) corresponds to the assignment of spin $1/2$ to the members of the original quark pair and is inconsistent with an integral spin assignment. This is shown quite strikingly in Figure 23.

VI. OTHER CHARMONIUM STATES

The above description reflects a rather satisfactory basis for understanding those members of the charmonium family, the psions, which have the same quantum numbers as the photon. Let us now examine what evidence we have for other members of that family. The general hope is that charmonium might play the same role in understanding quark dynamics that the hydrogen atom has played in understanding quantum electrodynamics. Since we are dealing with relatively heavy quarks at moderate excitations, one can even hope that purely non-relativistic considerations may give a fair description. Figure 24 is a diagram of the theoretically expected states of charmonium projected on that basis. The question is whether the various states shown in this figure correspond to reality. As we shall discuss, the answer to this question is again "yes," with some experimental uncertainty remaining in respect to the two pseudo-scalar states, that is the spin-0 objects with negative intrinsic parity.

In Figure 25 we show the spectrum based on actual experimental results. There indeed appear to be three 3P states called the χ -particles which can be fed by electric dipole γ -ray transitions from the ψ' . The experimental evidence for the existence of these three states is now very firm. Direct observation of the monochromatic γ -rays feeding these states has been made by the use of small sodium iodide detectors surrounding one of the interaction regions of SPEAR. Spectra taken at the ψ' and a "control" at the J/ψ peak are shown in Figure 26. The photons have also been seen by observation of electron-positron pairs originating from conversion of the γ -rays. The states can be isolated by examining the hadron decay spectra of those events which are in coincidence with photons of various energies, and the branching ratios corresponding to electromagnetic decays of these states can be determined. Let me add that the earlier detectors used in connection with electron-positron annihilation were not specifically designed with good efficiency and resolution for high-energy photons, and therefore it is expected that much better data on this subject will be forthcoming in the near future as several newer instruments become dedicated to γ -ray spectroscopy.

Figure 27 is a scatter plot of events from several experiments in which a state intermediate between the ψ' and the ψ/J is being fed by a photon and a further photon is subsequently emitted. It is relatively easy from this chart to determine which photon is the one which feeds the state and which one originates from subsequent photon emission because the latter photon line is Doppler-broadened due to the recoil of the intermediate state. Evidence seems to be good that intermediate states indeed exist at energies of 3.550, 3.510, 3.455 and 3.415 GeV. The question is which of these is which - that is, what are the term assignments? We can begin by ruling out 0^- and 1^+ assignments for the 3.415 state since it is observed to decay into $\pi^+\pi^-$ and K^+K^- states which would be forbidden under this assignment. Accordingly, the 3.415 state must be either the 0^+ or the 2^+ state. As is shown in Figure 28, the angular distribution of the photons appears to be consistent with $1 + \cos^2\theta$ which fits the 0^+ but not the 2^+ assignment. Thus the 3.415

GeV state is 0^+ , the lowest member of the triplet, and we assume that the 3.510 and 3.550 states are the two higher members. Their angular distributions are consistent with that assignment, as Figure 29 specifically shows for the 3.510 state, and it appears logical that their masses should be in the natural order. It is also reassuring to note that the branching ratios for transitions from the ψ' to the three intermediate 3P states are comparable.

The branching ratio for transition from the ψ' to the 3.455 GeV state is much smaller, so small in fact that it is not evident in the inclusive γ -ray spectra. One can therefore conclude that it is not a member of the 3P triplet, but that it might be the pseudo-scalar singlet 2^1S_0 (0^-). Additional confirmation that the 3.510 GeV state is in fact the 1^+ member of the 3P triplet is obtained from the apparent suppression of its hadronic decays relative to the other states. This complex situation is summarized in Figure 30.

For all these reasons the term assignments for the 3P states appear to be made with reasonable confidence. However, the evidence for the existence of the ground state of the pseudo-scalar member of charmonium, which is believed to be near 2.8 GeV, is not fully firm. Experience at DESY in the decay of the ψ/J into three γ -rays has shown that the effective mass of pairs of γ 's appears to peak at an energy near 2.8 GeV. This is best interpreted by assuming that the ψ/J decays with emission of a single γ -ray into the 2.8 GeV pseudo-scalar state, which subsequently decays into a pair of photons.

The branching ratios for decays into the pseudo-scalar states are thus far in poor agreement with theory, as is the location of the 2.8 GeV state. This side of charmonium spectroscopy is still in need of clarification. However, as an overall assessment it is certainly extraordinary how satisfactory the agreement between theory and experiment appears to be and how rapidly a complete spectroscopy has evolved in this new field while ordinary meson spectroscopy has taken more than a decade to evolve and still has many unsatisfactory points remaining.

We thus conclude that charmonium spectroscopy, that is the spectroscopy of new mesons involving the charmed quark but having net charm quantum number 0 is in relatively good shape. We do, of course, also expect combinations of the charmed and ordinary quarks leading to what is known as charmed particles, that is, both mesons and baryons of total charm quantum number different from zero. We will now discuss the evidence for such "charmed" particles.

VII. CHARMED PARTICLES

The masses of the quarks can be roughly estimated by assuming that they are only very weakly bound with their antiparticles in forming the lightest vector mesons. The resulting mass estimates are shown in Figure 31. Accordingly, the lightest charmed particles should be $c\bar{u}$ or $c\bar{d}$ mesons having a mass somewhat below $1.55 + 0.39 = 1.94$ GeV. On this basis it appears reasonable that the ψ' peak at 3.684 GeV is below threshold for forming a pair of charmed particles, while the broader peaks at 3.77 GeV and higher are above that threshold. Thus the most likely region to hunt for charmed particles might well be at the peaks of these broader structures.

Experimental identification of charmed particles has to proceed through analysis of their decays via the weak interaction. Since charm is presumably a quantum number that is conserved in the strong interaction, a charmed particle can only convert into another charmed particle if strong decays are involved. In contrast, weak decays can change the hadronic quantum numbers of charm, strangeness, isotopic spin, etc., according to certain rules. The charm quantum number has been incorporated into the theory of weak decays, and in fact one of the incentives for the suggestion of charm was that by adding a fourth quark a great deal of symmetry could be restored to the formalism which governs the behavior of weak decays. Unfortunately I cannot go into this subject here beyond the barest outline.

Certain selection rules have been experimentally established which show that some quantum numbers change easily under weak decays, while others are inhibited by a substantial factor. Theory accommodates this fact by the introduction of the so-called Cabbibo angle, whose cosine connects amplitudes where transitions are likely, and whose sine connects amplitudes

where transitions are inhibited. In consequence, the ratio of so-called "Cabbibo-forbidden" to "Cabbibo-allowed" decays is the square of the tangent of the Cabbibo angle, which numerically is about 6%. When the charm quantum number is incorporated into the overall scheme of the weak interaction in the most symmetric manner, then the Cabbibo-allowed transitions require that the charm quantum number be converted into the strangeness quantum number (the latter has been known and used in particle physics for well over a decade). Accordingly, the signature of a charmed decay is that it results in combinations of strange and non-strange particles. In the case of the lightest charmed meson, the expected decay would be into a kaon and a pion. The selection rules "allowing" the decay of a charmed meson into another hadron and a pair of leptons demand that, for the hadron, $\Delta Q = \Delta S = \Delta C$ where Q, S, and C are charge, strangeness and charm, respectively; in addition, change in isotopic spin is forbidden.

Guided by these rules, a worldwide search for charmed particles took place which finally culminated in their successful discovery at SPEAR. The problem had been in earlier work at SPEAR that discrimination between charged π 's and K's had been difficult with the existing detectors, and an elaborate analytical procedure had to be developed to sharpen up this discrimination within the information available which consisted of time-of-flight measurements over a path length of approximately $1\frac{1}{2}$ meters. Figure 32 shows the effective mass spectra of various particle combinations observed in e^+e^- annihilation. It can be seen from the figure that the $K\pi$ and $K3\pi$ combinations exhibit peaks, while the remaining combinations (4π and $2K2\pi$) do not. Similar results for the charged channels, shown in Figure 33, indicate peaking in the so-called exotic combinations

$$K^-\pi^+\pi^+ \text{ and } K^+\pi^-\pi^-$$

but not in the non-exotic $K^-\pi^+\pi^-$ and $K^+\pi^-\pi^+$. Analysis of the events contained within these peaks in the mass spectra has also shown that the effective mass of the remaining particles in the event - the recoil mass system - is

at least as large as that of the resonant peak combinations themselves. This is strong evidence for the view that the process being observed is pair production of heavy objects having a new quantum number (thus the need for pairs).

The common interpretation of these findings was that the lowest-mass charmed particles, the D mesons, were indeed being produced in both charged and neutral forms, and also in both the ground and first-excited states (D^*). More detailed analyses of the recoil spectra have amply confirmed this view, and a fortuitous combination of circumstances has subsequently made it possible to determine the masses of each of the observed D mesons with quite remarkable accuracy. In Figure 34 we show the spectra of the charmed mesons as calculated theoretically, with the present experimental mass values added to the diagram.

The unusual accuracy of these mass determinations is connected with the fact that the complex recoil spectra that are produced in combination with the formation of, say, a D^0 meson can reveal a great deal of detail about the channels in which the D^0 was formed. This point is illustrated in Figure 35, which shows the various contributions that are expected to the D^0 momentum spectrum near threshold, and also the observed spectrum for $D^0 \rightarrow K^- \pi^+$ at $E_{cm} = 4.028$ GeV. The masses of the D^* and D states are such that the transition can occur through either pion or gamma-ray emission. This enables not only masses but also branching ratios to be determined to good precision.

The picture which evolves out of all this is that there does indeed exist a threshold of about 3.73 GeV below which a pair of charmed mesons cannot be created, but below which the psions which are composed of bound charmed quarks with their antiparticle can be formed. The option to decay into charmed objects, then, is the main factor in determining the structure of the positron-electron annihilation cross section above charm-pair production threshold.

This interpretation has been reinforced by the recent discovery of a peak at 3.77 GeV, less than 100 MeV above the ψ' (3684). The 3.77 peak is thus just barely above the threshold for pair production of the $D^0\bar{D}^0$ and also D^+D^- but not with their excited states. Therefore the 3.77 GeV peak constitutes an ideal "laboratory" for examining the properties of the D particles under background-free conditions. Note that at higher energies pure $D^0\bar{D}^0$ production is suppressed in the more complex pattern discussed previously and shown in Figure 35. Again I cannot go into detail here, but the fortuitous existence of the 3.77 GeV peak has made it possible to sharpen up the mass determination of the D^0 even further and to allow a systematic tabulation of the D^0 decay modes. Moreover, it promises to give statistically better useful spectra of the weak decay patterns of these new charmed objects.

In addition to the system of the four low-lying D particles which have been seen so far, and whose properties are quite well understood, one does, of course, expect an expanded spectroscopy of higher excited states. One also expects the existence of the so-called F mesons, which are a combination of the charmed quark and a strange rather than an ordinary quark. The D and F mesons are compared in Figure 36. Recent evidence from DESY has given a hint that the F particles may indeed exist; the $\eta\pi$ combination observed there is a rather characteristic signature for the existence of the F.

It is also expected that not only a spectroscopy of charmed mesons but also of charmed baryons should exist. These objects presumably consist of triplets of quarks at least one of which is charmed. The hunt for these particles thus far has been beset with difficulties. Fairly persuasive evidence as to their existence came from an experiment by Won-Yon Lee and collaborators at Fermilab, where a peak at 2.25 GeV in the effective mass combination of an anti- Λ particle associated with three mesons was seen with impressive statistics. This object may be the decay product of the otherwise difficult to explain events seen in earlier bubble chamber experiments at Brookhaven. However, although an anti-charmed baryon apparently has been seen, the hunt for its charge-conjugate has thus far been unsuccessful.

Quite persuasive indirect evidence for the existence of a charmed baryon has very recently been observed at SPEAR. If the proton or antiproton combined inclusive yield is examined as a function of electron-positron annihilation energy, this quantity appears to double between center-of-mass energies of about $4\frac{1}{2}$ and 5 GeV; the yield of $\Lambda\bar{\Lambda}$ pairs also increases in this region but not so rapidly. Although any detailed interpretation would be premature, this observation seems to indicate that there is indeed an onset of the production of new, and presumably charmed, baryon-antibaryon pairs, but that these objects decay preferentially into proton-antiproton combinations rather than combinations of strange baryons, such as the Λ or Σ . This may explain why the hunt for charmed baryons decaying into strange baryons, which was believed to be the most characteristic signature of charmed baryons, has been so difficult.

VIII. OVERVIEW

To summarize, the physics underlying most (but not all!) of the complex structure of the electron-positron annihilation cross-section as a function of energy appears to be understood generally in terms of various thresholds and the resultant production of combinations of charmed mesons, of psions, and probably also of charmed baryons. However, there is room - and in fact evidence - for more. To begin with, there are highly persuasive data that I will not discuss here, which indicate the existence of leptons heavier than the electrons, neutrinos and muons. Evidence for these heavy leptons (mass around 1.9 GeV) was first collected by Perl and collaborators, who observed that there was an excess of real coincidences of electrons and muons that appeared as products of electron-positron annihilation. Supporting data have been generated at DESY. The excitation and spectra of these electrons and muons are difficult to account for through any mechanism other than that they are the decay products of heavier members of the lepton family. A second important result is the recent discovery at Fermilab that the effective mass spectra of muon pairs generated from nucleon-nucleon collisions exhibit a multi-peak structure at an effective mass

above 9.5 GeV. This most recent observation gives us a strong signal that the up and down quarks and the strange and charmed quarks may not constitute the full membership of the quark family, but rather the conjectured "truth and beauty" quarks may not be far behind.

This summary of the experimental basis for the new spectroscopy thus has to conclude on a tantalizing note. Although it is certainly true that, starting from the November 1974 revolution, we have gained a remarkable understanding of the new spectroscopy involving charmed quarks in so short a time, we are now beginning to find that in spite of this understanding the future seems to be wide open to the possible existence of new members in both the quark and lepton families of elementary particles. It seems very likely that electron-positron storage rings in the next energy range will again prove to be the most powerful tools to look at this unfolding chapter.

Aside from establishing or denying the existence of the additional quarks and leptons, much remains to be done to solve the many puzzles still remaining within the now firmly established families of four quarks and four leptons (e, ν_e, μ, ν_μ). The situation concerning the pseudoscalar charmonium states is still unsatisfactory, the evidence on the charmed-strange mesons is highly tentative, and the charmed baryon picture is just beginning to emerge. Quantitatively there remain many discrepancies between observed transition rates and calculations. However, these open questions notwithstanding, the new quark spectroscopy already presents an amazingly complete and consistent pattern, considering the short time span of its existence. The profound problems - the description of quark dynamics and the mechanism of their confinement - remain in a tentative state.

Symbol	Q	I_3	C	Y	S
u (or p)	2/3	1/2	0	1/3	0
d (or n)	-1/3	-1/2	0	1/3	0
s (or λ)	-1/3	0	0	-2/3	-1
c (or p')	2/3	0	1	-2/3	0

Fig. 1

Quarks and their quantum numbers in SU(4).

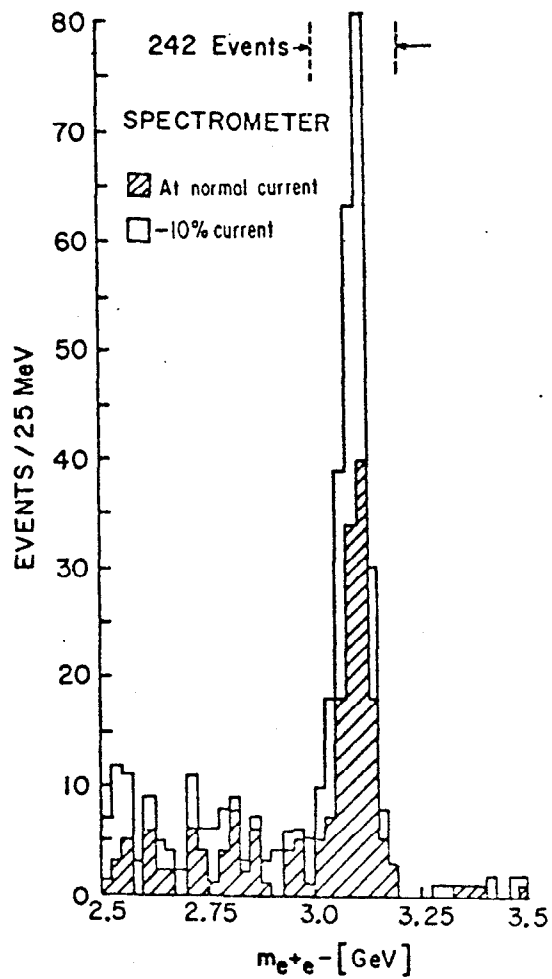


Fig. 2

The $J/\psi(3095)$ resonance as measured at Brookhaven National Laboratory by a joint MIT-Brookhaven group.

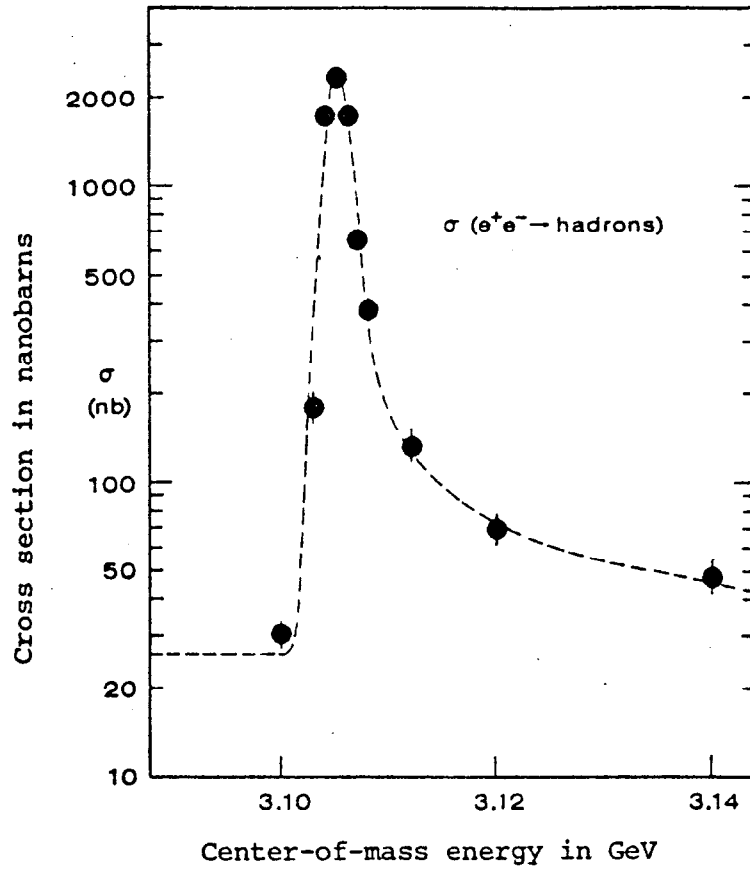


Fig. 3

The $\psi/J(3095)$ resonance as measured at the SPEAR electron-positron storage ring by a joint group from SLAC and Lawrence Berkeley Laboratory.

$$\Gamma_{e^+e^-} = \left(\frac{m^2}{6\pi^2} \right) \int \sigma_{\text{total}} dE$$

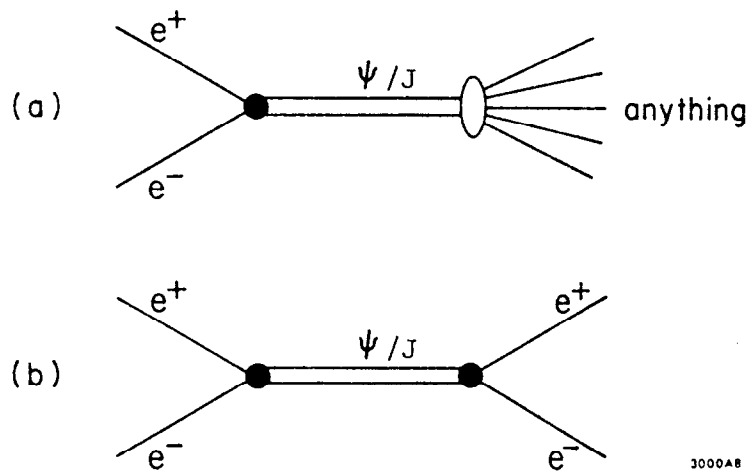


Fig. 4

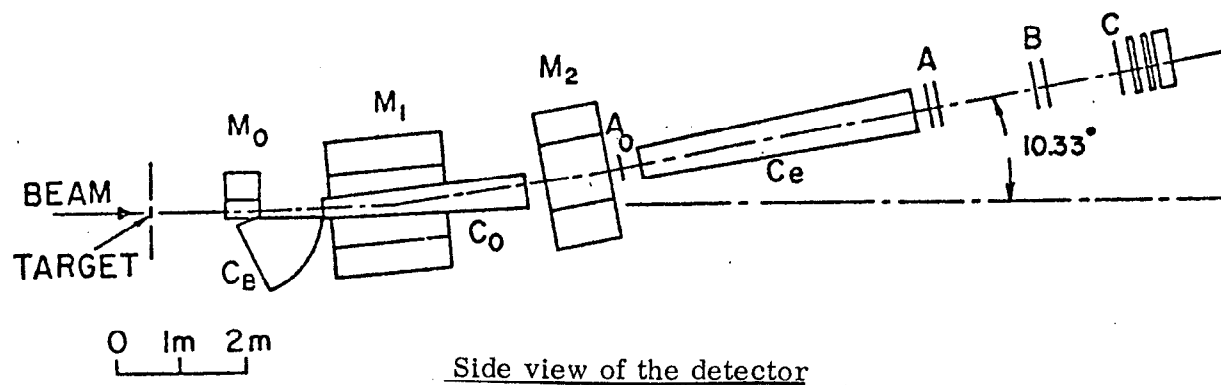
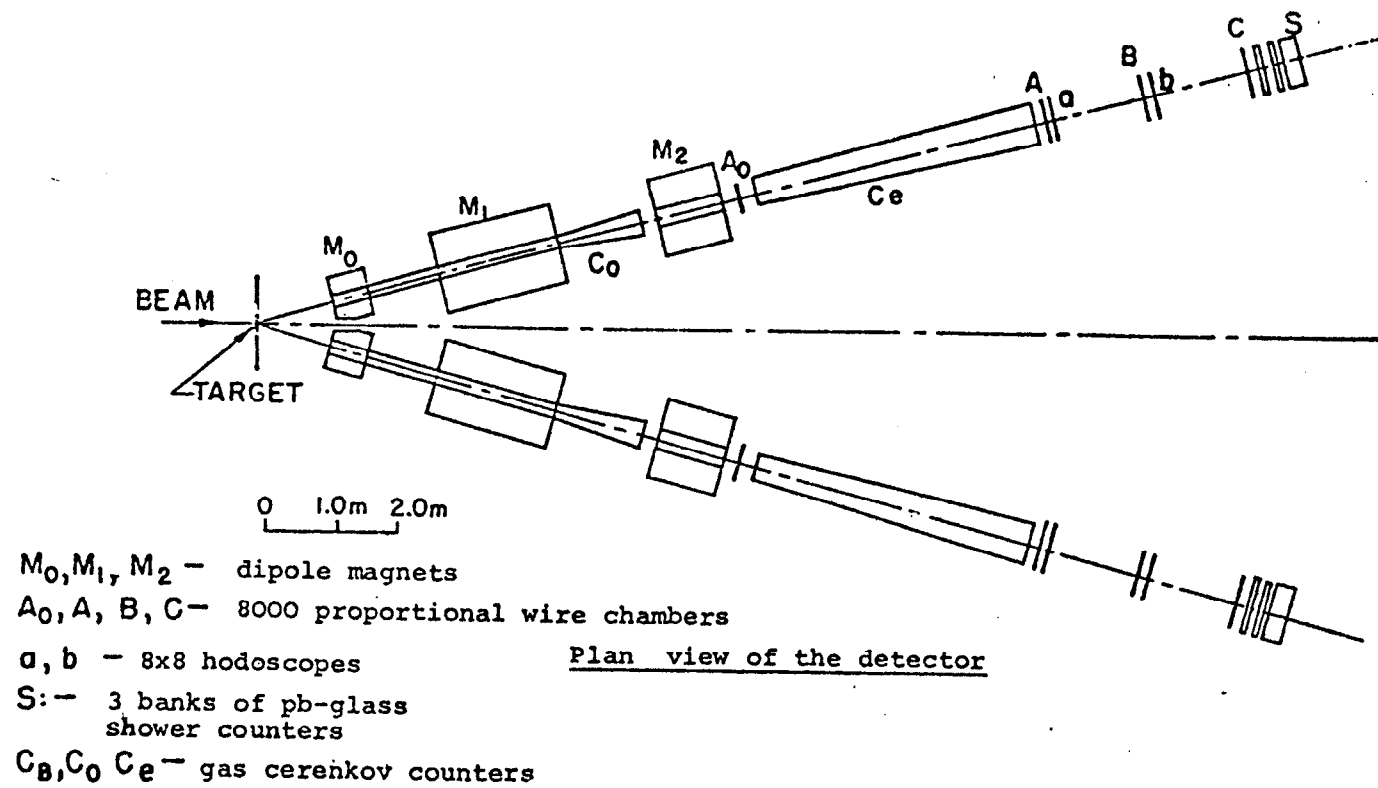


Fig. 5

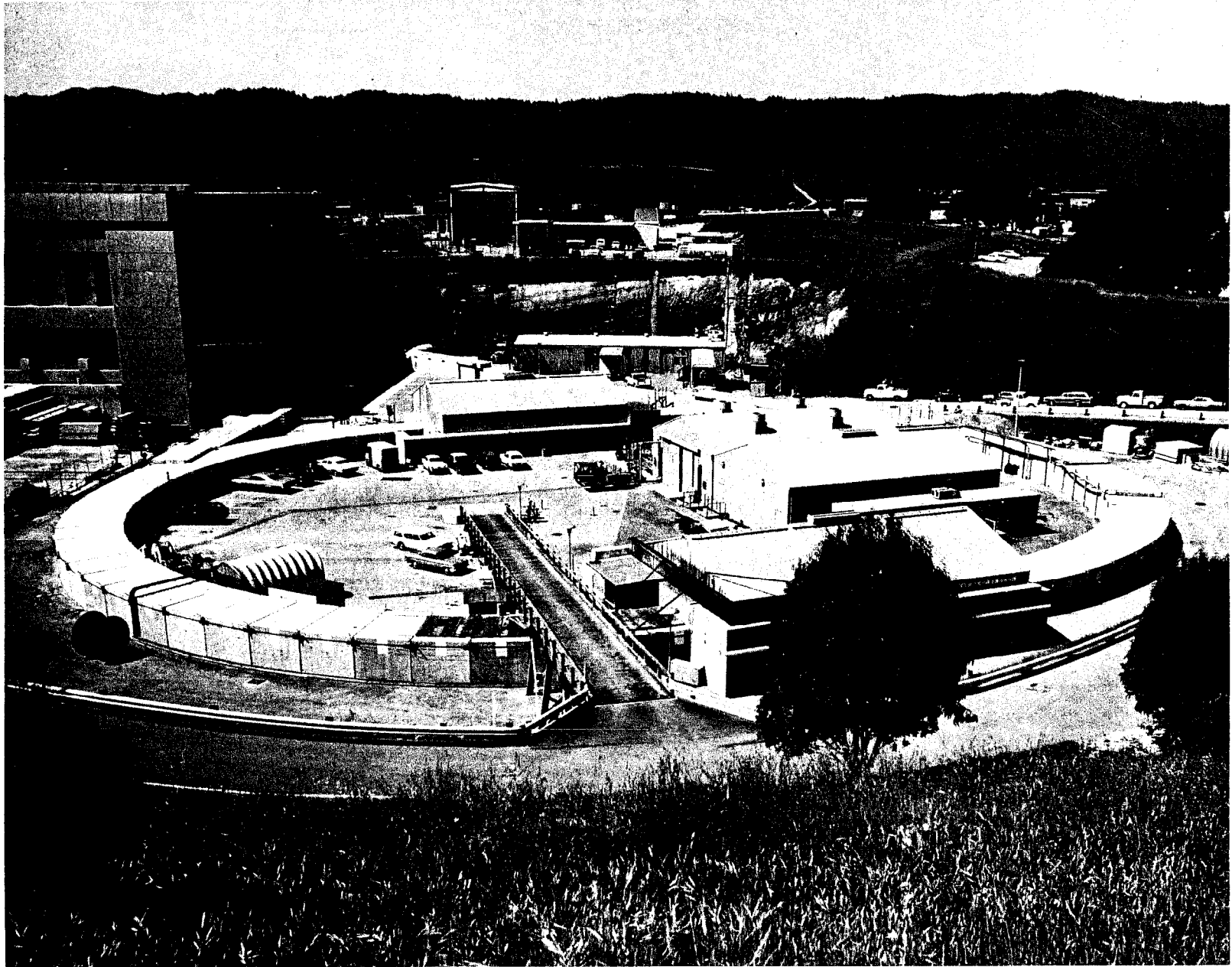
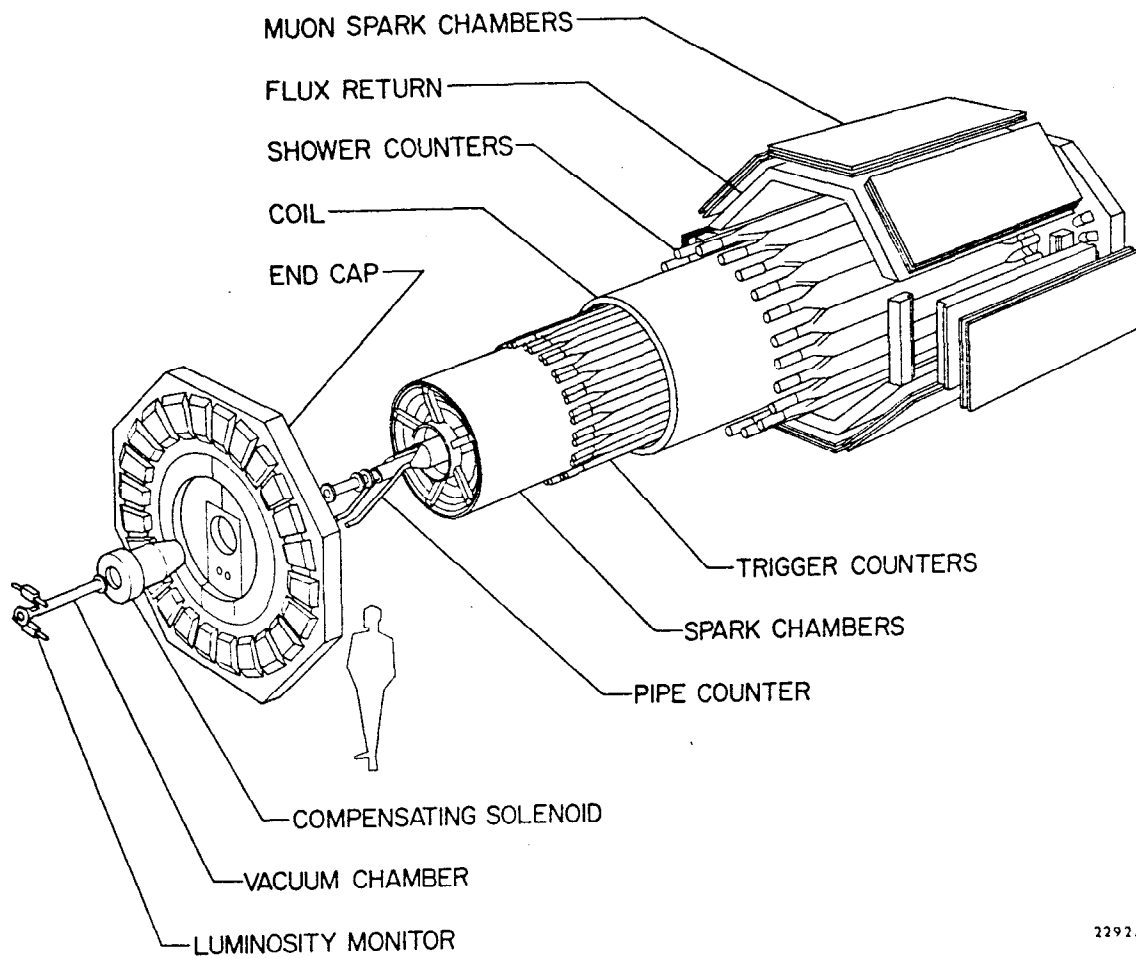


Fig. 6



2292A1

Fig. 7--A telescoped view of the Mark I detector used at the SPEAR storage ring at SLAC.

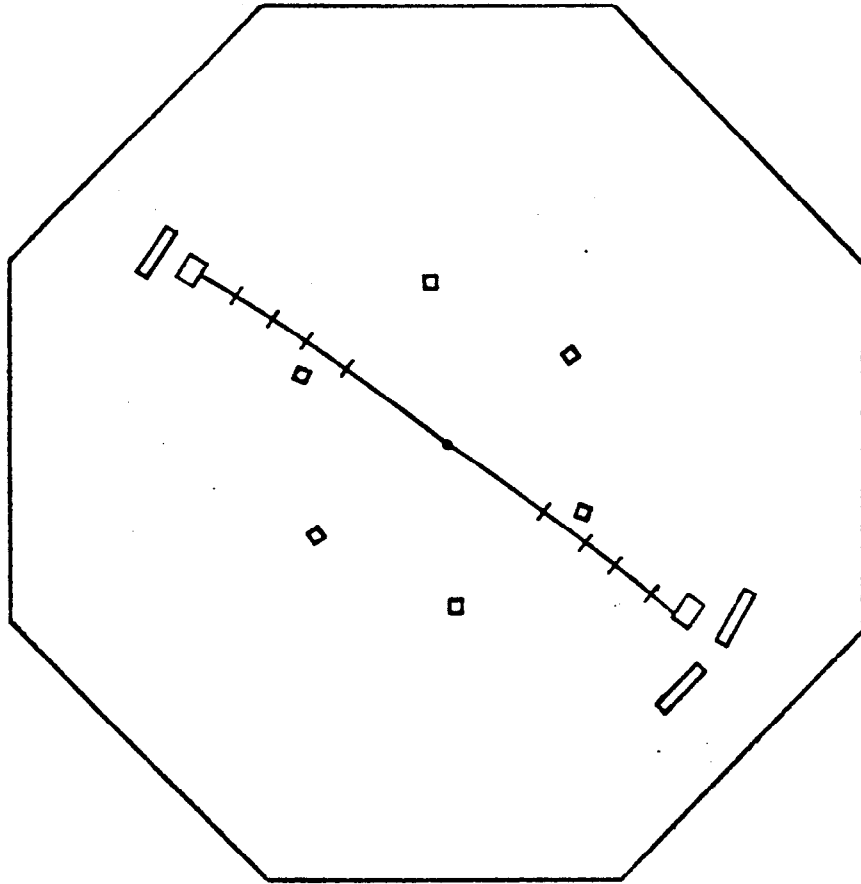


Fig. 8--An event in which two charged particles emerge collinearly from the interaction region. More information is needed to distinguish the more likely reactions

$$e^+e^- \rightarrow e^+e^-, \quad e^+e^- \rightarrow \mu^+\mu^-$$

from the less likely creation of charged hadron pairs:

$$e^+e^- \rightarrow p\bar{p}, \quad K^+K^-, \quad \text{etc.}$$

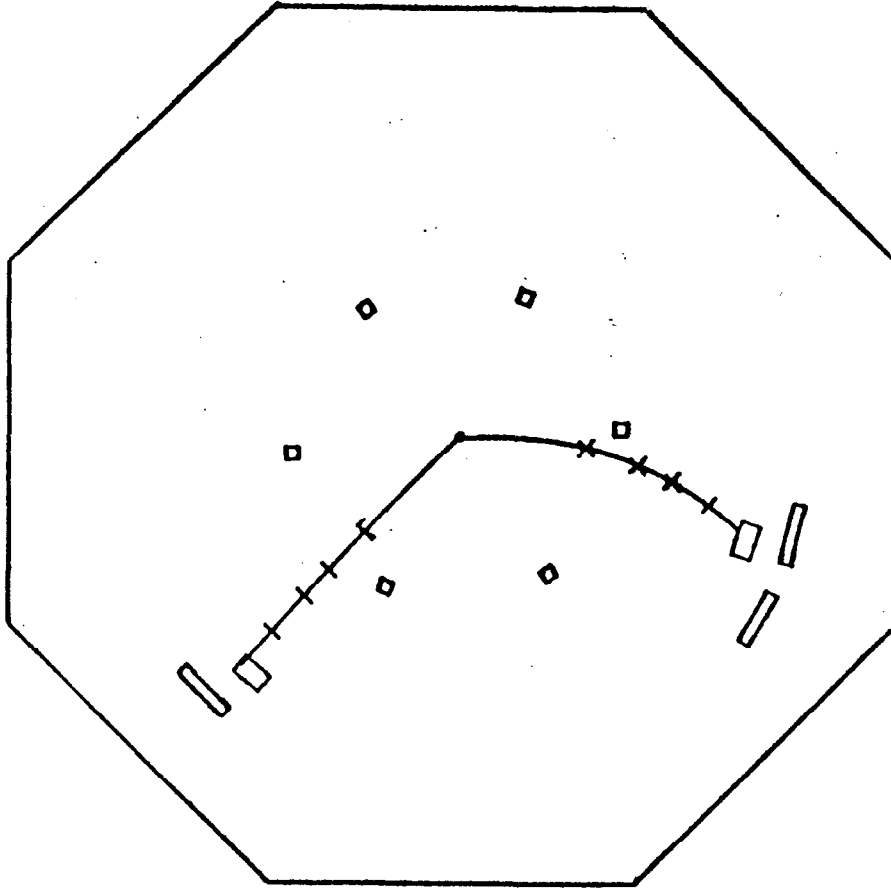
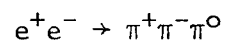


Fig. 9--Observation of two non-collinear charged particles indicates at least one undetected neutral particle in the event. For example:



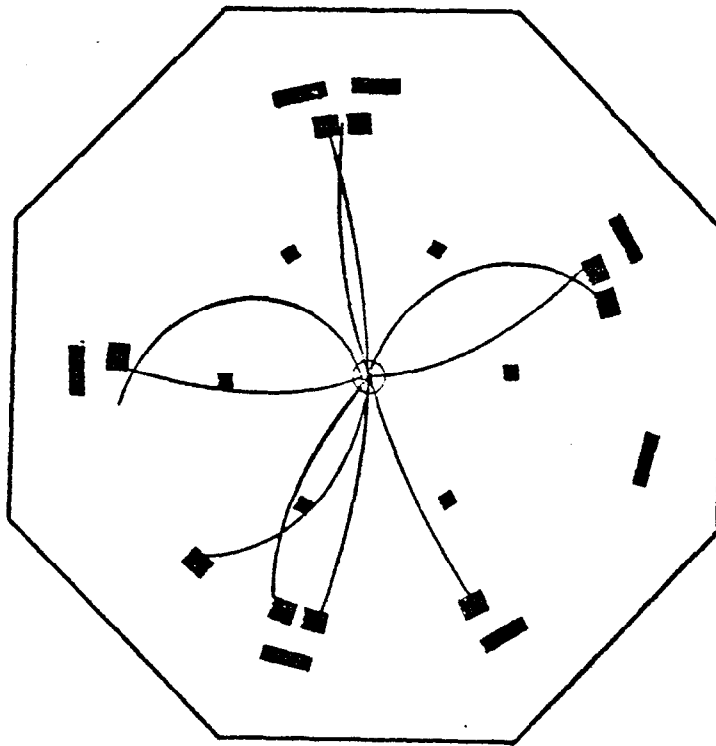
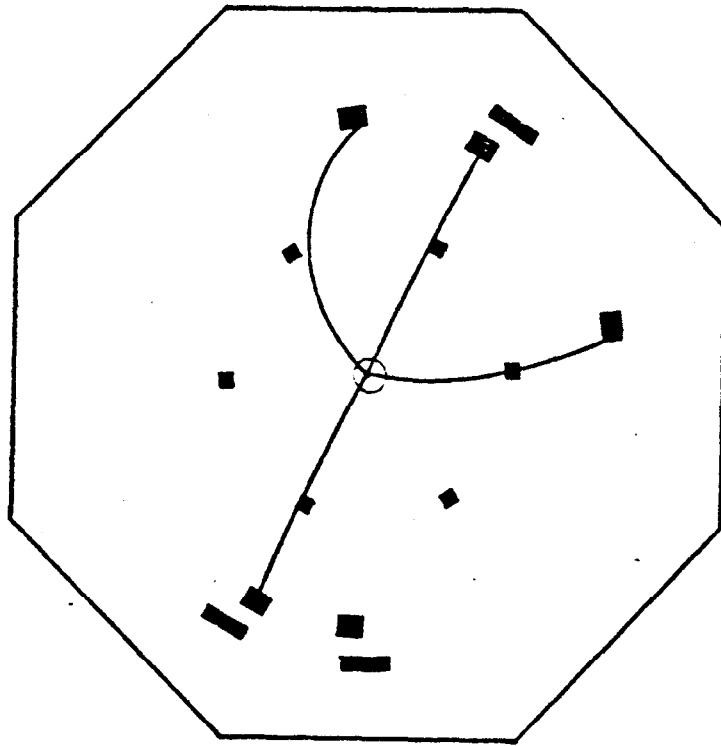
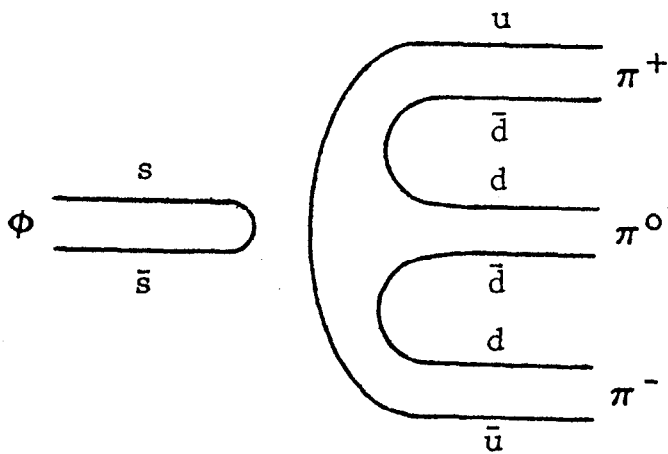
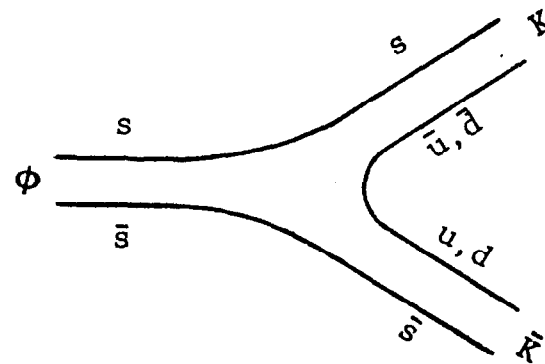


Fig. 10--Two examples of multihadronic events recorded at SPEAR.



$\phi \rightarrow 3\pi$
Forbidden



$\phi \rightarrow K\bar{K}$
Allowed

Fig. 11 -- Phi meson decay modes.

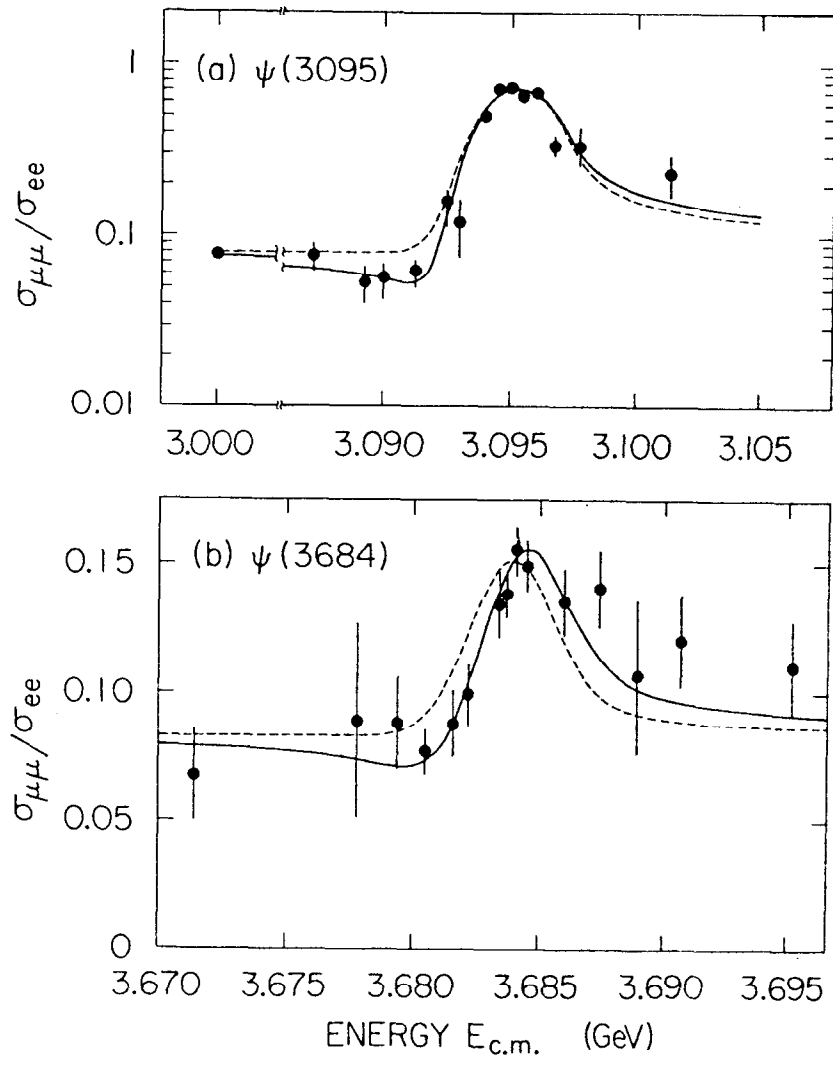


Fig. 12

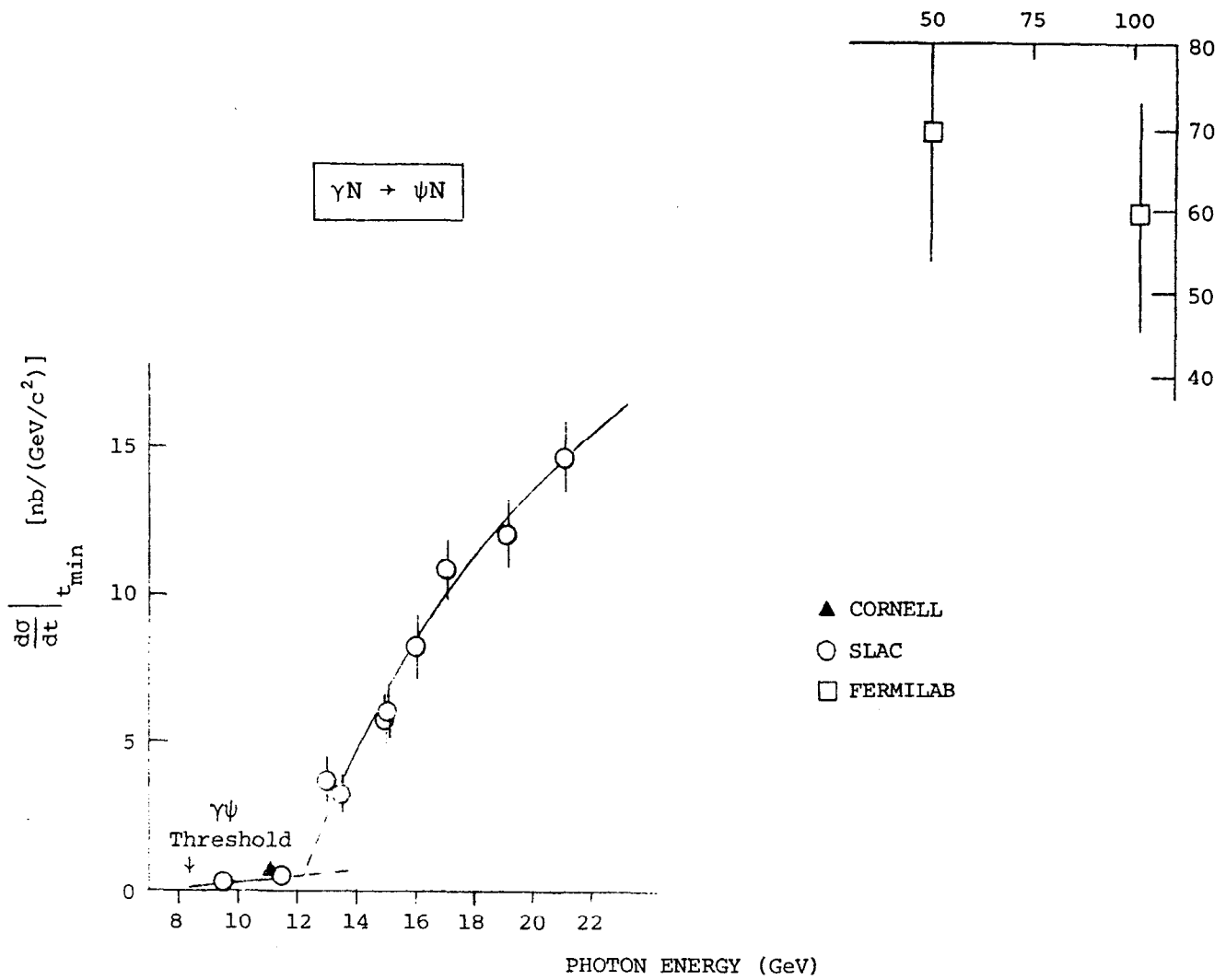


Fig. 13--Psi photoproduction.

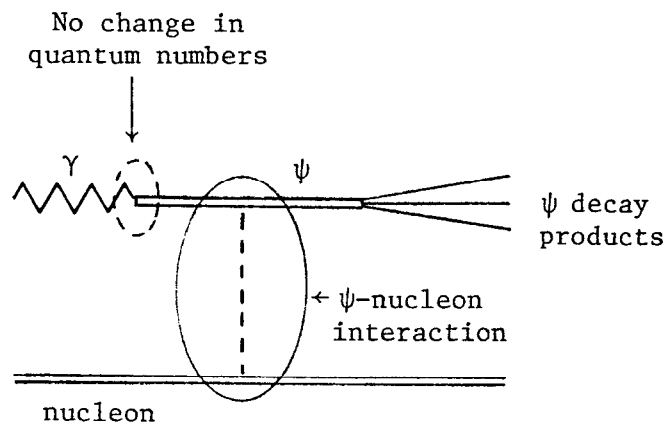


Fig. 14--Diffractive photoproduction of psions.

Mode	Fraction (%)	Mode	Fraction (%)
$e^+ e^-$	7.3 ± 0.5	$\phi \pi \pi$	0.21 ± 0.09
$\mu^+ \mu^-$	7.5 ± 0.5	ϕf	<0.037
$\pi^+ \pi^-$	0.011 ± 0.006	$\phi 2\pi^+ 2\pi^-$	<0.15
$\pi^+ \pi^- \pi^0$	1.6 ± 0.6	$\omega K \bar{K}$	0.16 ± 0.10
$2\pi^+ 2\pi^-$	0.4 ± 0.1	$\omega f'$	<0.016
$2\pi^+ 2\pi^- \pi^0$	4.3 ± 0.5	$\phi K \bar{K}$	0.18 ± 0.80
$3\pi^+ 3\pi^-$	0.4 ± 0.2	$\phi f'$	0.08 ± 0.05
$3\pi^+ 3\pi^- \pi^0$	2.9 ± 0.7	$\phi \eta$	0.10 ± 0.06
$4\pi^+ 4\pi^- \pi^0$	0.9 ± 0.3	$\phi \eta'$	<0.13
$\rho \pi$	1.12 ± 0.15	$p \bar{p}$	0.21 ± 0.02
$A_2^+ \pi^-$	<0.43	$p \bar{n} \pi^-$	0.38 ± 0.08
$\omega \pi \pi$	0.82 ± 0.16	$p \bar{p} \pi^0$	0.10 ± 0.02
ωf	0.28 ± 0.11	$p \bar{p} \eta$	0.19 ± 0.04
$B \pi$	0.38 ± 0.09	$p \bar{p} \pi^+ \pi^-$	0.41 ± 0.08
$\rho \pi \pi \pi$	1.8 ± 0.45	$p \bar{p} \pi^+ \pi^- \pi^0$	0.11 ± 0.04
ρA_2	0.84 ± 0.45	$p \bar{p} \omega$	0.05 ± 0.01
$\omega 2\pi^+ 2\pi^-$	0.85 ± 0.34	$\Lambda \bar{\Lambda}$	0.16 ± 0.07
$K^+ K^-$	0.017 ± 0.011	$\Lambda \bar{\Xi}$	<0.04
$K_S K_L$	<0.0089	$\Xi^- \bar{\Xi}^-$	~ 0.04
$K_S K^- \pi^+$	0.26 ± 0.07	$\Upsilon \Upsilon$	< 0.05
$K^+ K^- \pi^+ \pi^-$	0.72 ± 0.23	$\Upsilon \pi^0$	0.0073 ± 0.0047
$K^+ K^- \pi^+ \pi^- \pi^0$	1.2 ± 0.3	$\Upsilon \eta$	0.088 ± 0.019
$K^+ K^- 2\pi^+ 2\pi^-$	0.31 ± 0.13	$\Upsilon \eta'$	0.24 ± 0.06
$2K^+ 2K^-$	0.07 ± 0.03	$\Upsilon X(2830)$	<1.7
$K^+ K^{*-}$	0.34 ± 0.05	$\Upsilon X(2830) \rightarrow 3\gamma$	0.013 ± 0.004
$K^0 \bar{K}^{0*}$	0.27 ± 0.06	$\Upsilon X(2830) \rightarrow \Upsilon p \bar{p}$	<0.004
$K^+ K^{*-**}$	<0.15	$\Upsilon \Upsilon \Upsilon$ (non-resonant)	<0.0078
$K^0 \bar{K}^{0***}$	<0.20		
$K^{0*} \bar{K}^{0*}$	<0.05		
$K^{0*} \bar{K}^{0**}$	0.67 ± 0.26		
$K^{0**} \bar{K}^{0**}$	<0.29		

Fig. 15--Decay modes of the $\psi(3095)$.

Mode	Fraction (%)	Mode	Fraction (%)
$e^+ e^-$	0.88 ± 0.13	$\gamma \gamma$	<0.5
$\mu^+ \mu^-$	0.88 ± 0.13	$\gamma \pi^0$	<0.7
$\psi \pi^+ \pi^-$	33.1 ± 2.6	$\gamma \eta$	<0.042
$\psi \pi^0 \pi^0$	15.9 ± 2.8	$\gamma \eta'$	<0.11
$\psi \eta$	4.1 ± 0.7	$\gamma \chi(2830)$	<1.0
$\psi \gamma + \psi \pi^0$	<0.15	$\gamma \chi(2830) \rightarrow 3\gamma$	<0.034
$\pi^+ \pi^-$	<0.005	$\gamma \chi(3415)$	7.3 ± 1.7
$2\pi^+ 2\pi^-$	0.08 ± 0.02	$\gamma \chi(3510)$	7.1 ± 1.9
$2\pi^+ 2\pi^- \pi^0$	0.35 ± 0.15	$\gamma \chi(3550)$	7.0 ± 2.0
$\rho \pi$	<0.1	$\gamma \chi(3455)$	<2.5
$K^+ K^-$	<0.005	$\gamma \chi(3455) \rightarrow \gamma \gamma \psi$	0.6 ± 0.4
$K^+ K^- \pi^+ \pi^-$	0.14 ± 0.04	$\gamma \chi(3455) \rightarrow 3\gamma$	<0.031
$p \bar{p}$	0.023 ± 0.007		
$\Lambda \bar{\Lambda}$	<0.04		
$\Xi^- \bar{\Xi}^-$	<0.02		

Fig. 16--Decay modes of the $\psi'(3684)$.

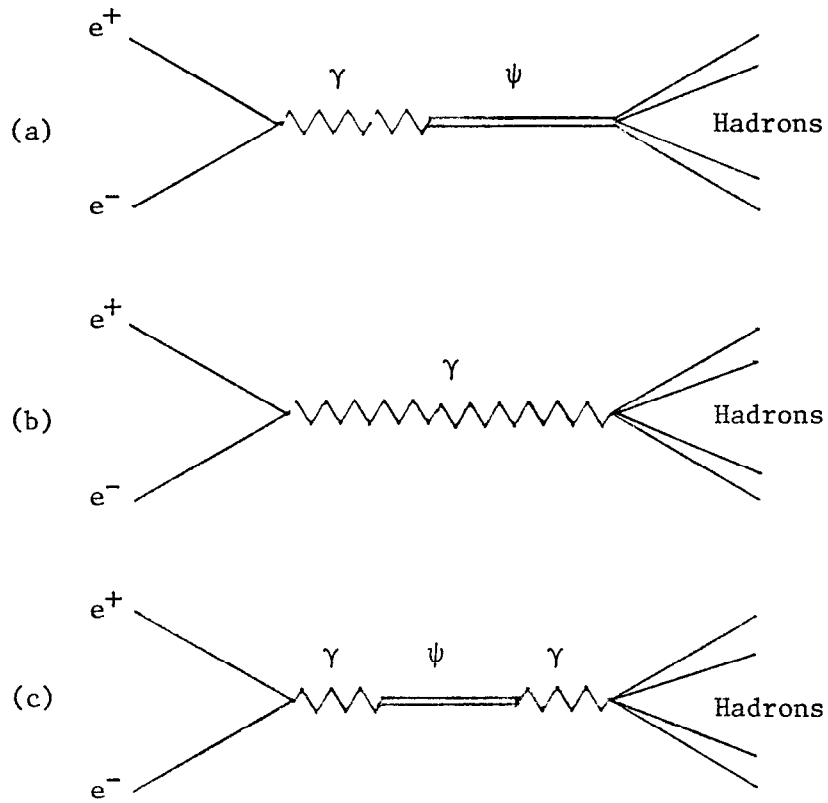


Fig. 17--Production of hadrons from e^+e^- annihilation via:
 (a) psi production and direct decay; (b) first-order
 electromagnetic production; (c) second-order electro-
 magnetic decay.

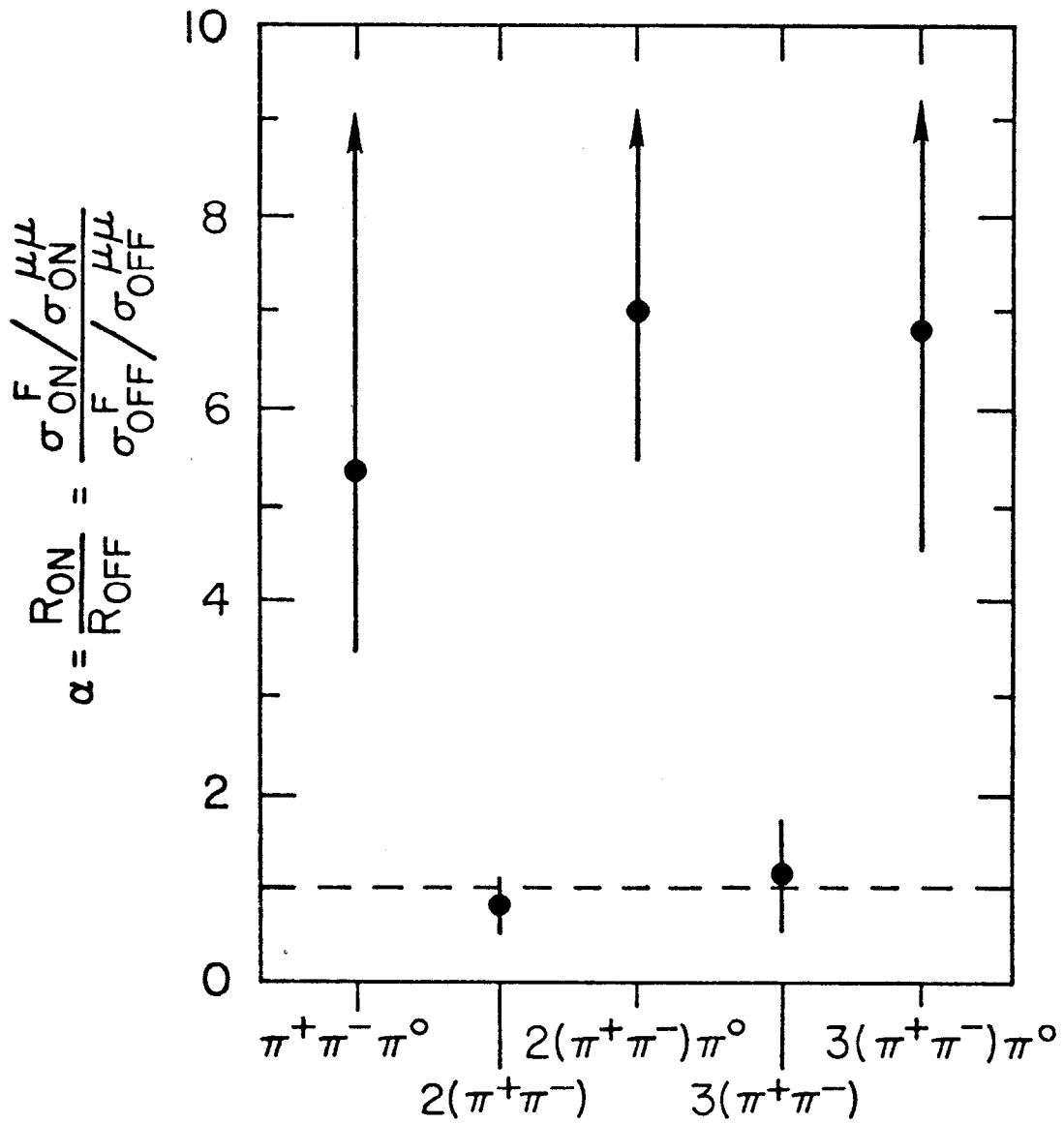


Fig. 18--Multipion decays of the $\psi(3095)$, illustrating the strong dominance of decays with an odd number of pions.

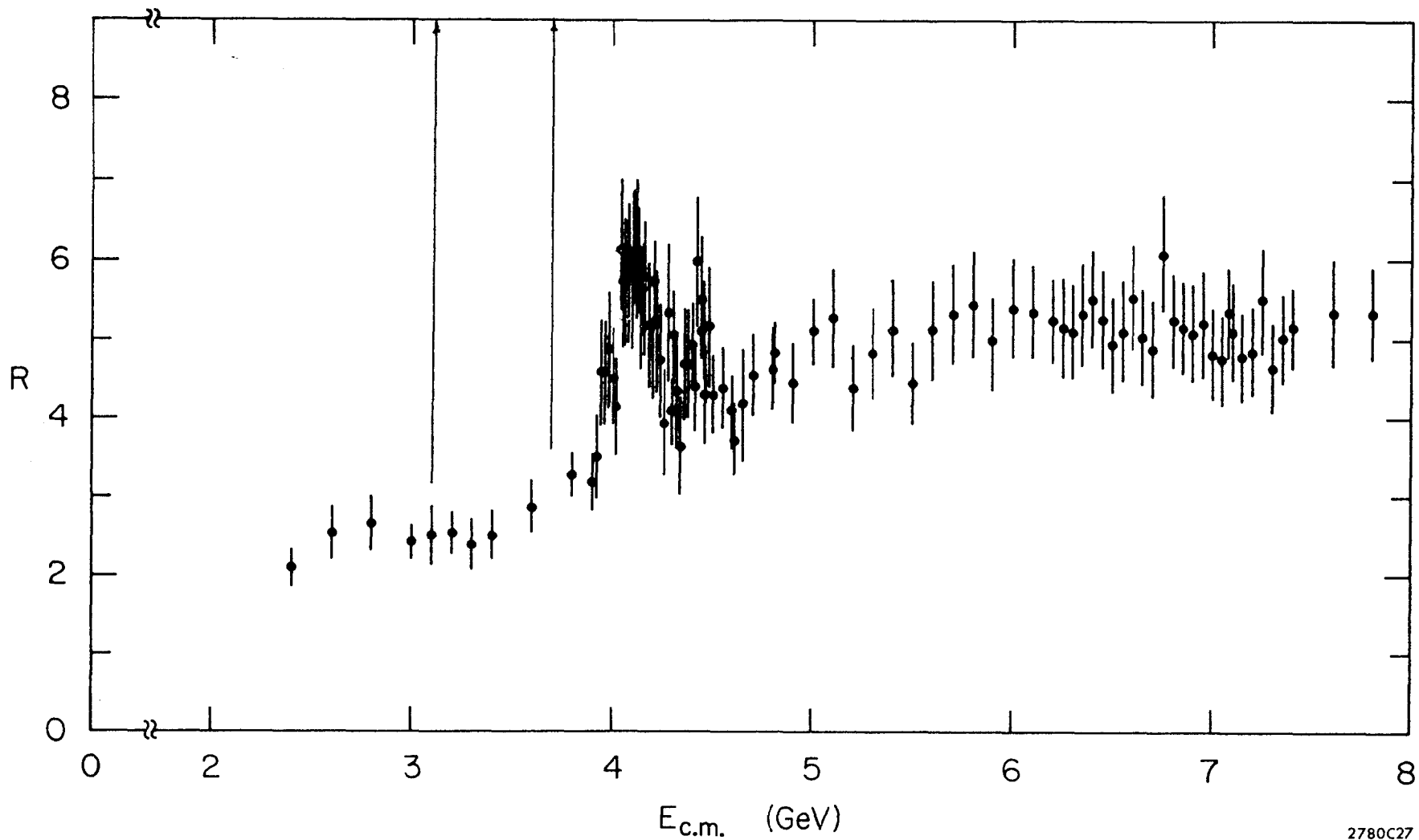


Fig. 19

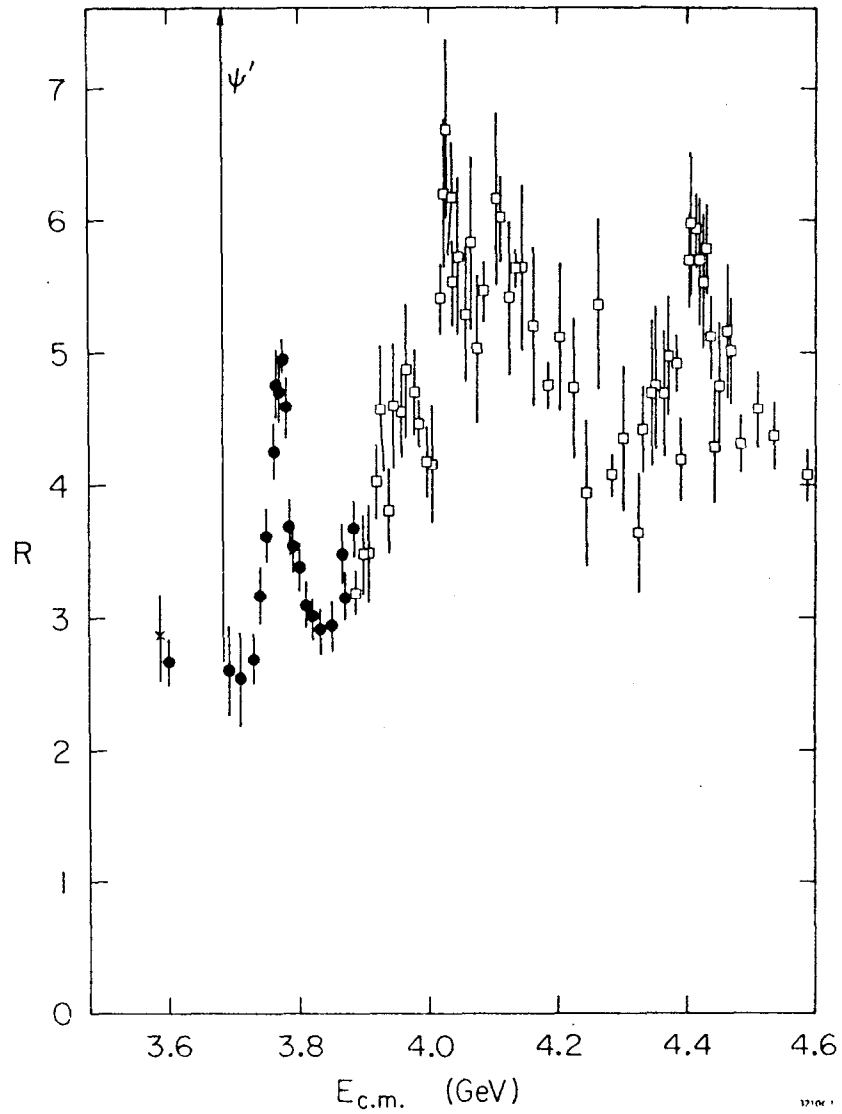


Fig. 20-- R vs. $E_{c.m.}$ in the complex transition region between 3.6 and 4.6 GeV. The resonant peak at 3.77 GeV is shown with black dots. Other structures at higher energies are described in the text.

$$R = \frac{\sigma_{e^+e^- \rightarrow \text{HADRONS}}}{\sigma_{e^+e^- \rightarrow \mu^+\mu^-}} = \left[\frac{\begin{array}{c} \text{e}^+ \quad \quad \quad \gamma \\ \quad \quad \quad \diagdown \quad \diagup \\ \quad \quad \quad \gamma \\ \quad \quad \quad \diagup \quad \diagdown \\ \text{e}^- \quad \quad \quad \text{HADRONS} \end{array}}{\begin{array}{c} \text{e}^+ \quad \quad \quad \gamma \\ \quad \quad \quad \diagdown \quad \diagup \\ \quad \quad \quad \gamma \\ \quad \quad \quad \diagup \quad \diagdown \\ \text{e}^- \quad \quad \quad \mu^+ \\ \quad \quad \quad \quad \quad \quad \mu^- \end{array}} \right]^2$$

$$= \left[\frac{\begin{array}{c} \text{e}^+ \quad \quad \quad \text{QUARKS} \\ \quad \quad \quad \diagdown \quad \diagup \\ \quad \quad \quad \gamma \\ \quad \quad \quad \diagup \quad \diagdown \\ \text{e}^- \quad \quad \quad \text{HADRONS} \end{array}}{\begin{array}{c} \text{e}^+ \quad \quad \quad \gamma \\ \quad \quad \quad \diagdown \quad \diagup \\ \quad \quad \quad \gamma \\ \quad \quad \quad \diagup \quad \diagdown \\ \text{e}^- \quad \quad \quad \mu^+ \\ \quad \quad \quad \quad \quad \quad \mu^- \end{array}} \right]^2 = \sum_i q_i^2 / e^2$$

Fig. 21--Significance of the ratio R.

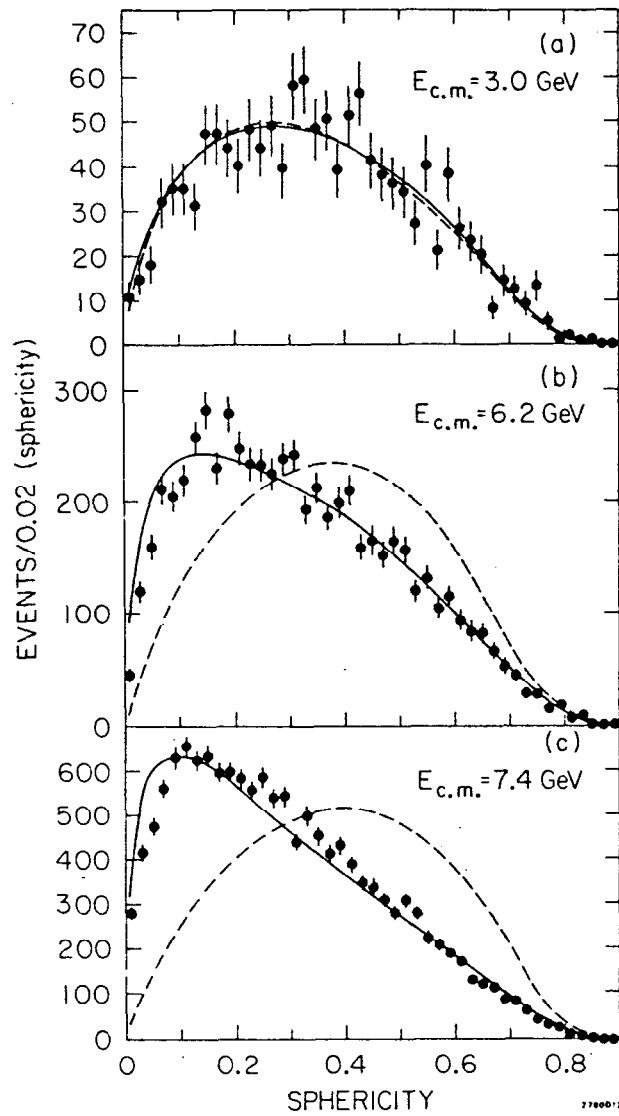
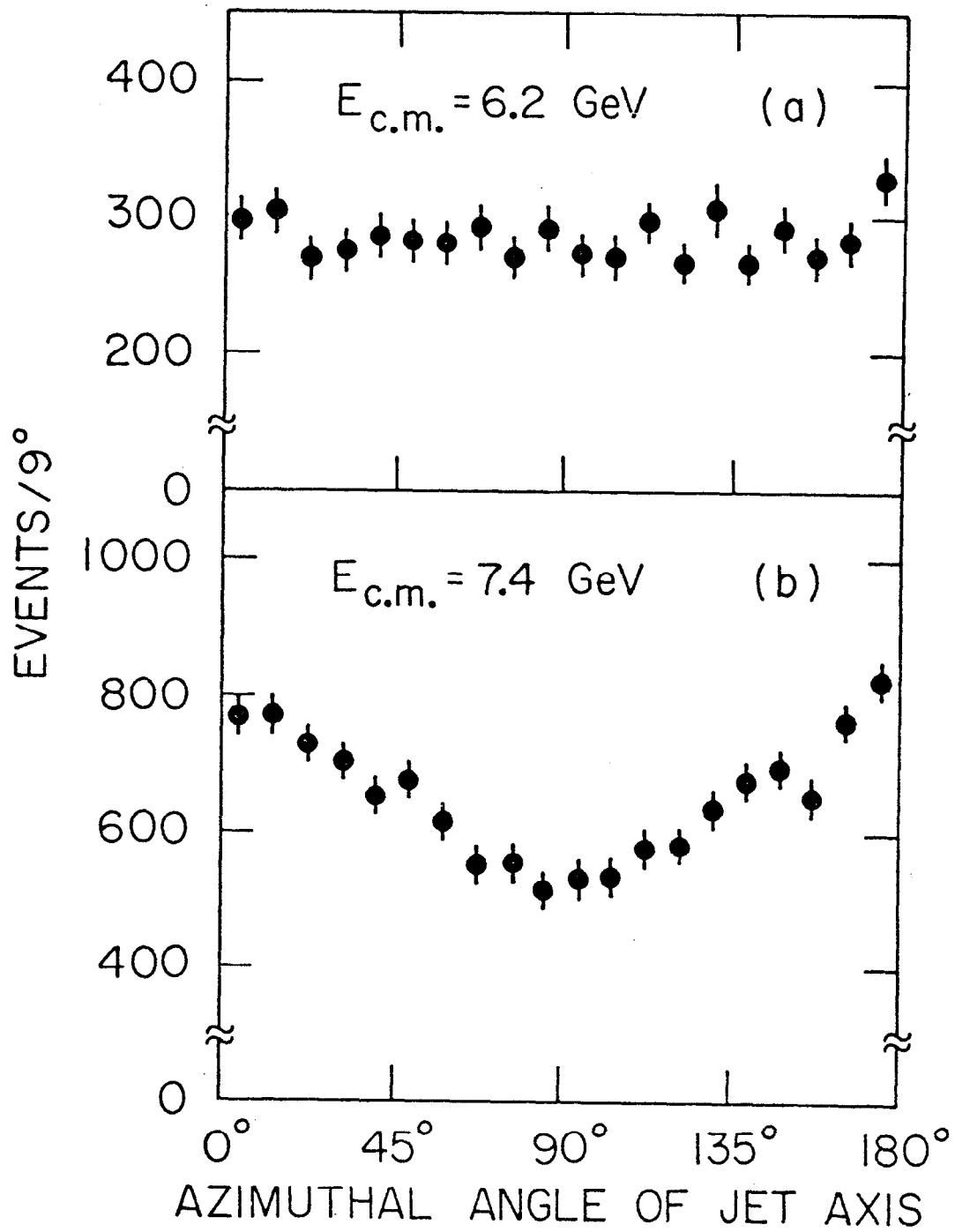


Fig. 22--"Sphericity" of the SPEAR events at three different center-of-mass energies. At the higher energies the tendency of the final-state particles to cluster about a "jet axis" becomes rapidly more pronounced.



2755A3

Fig. 23

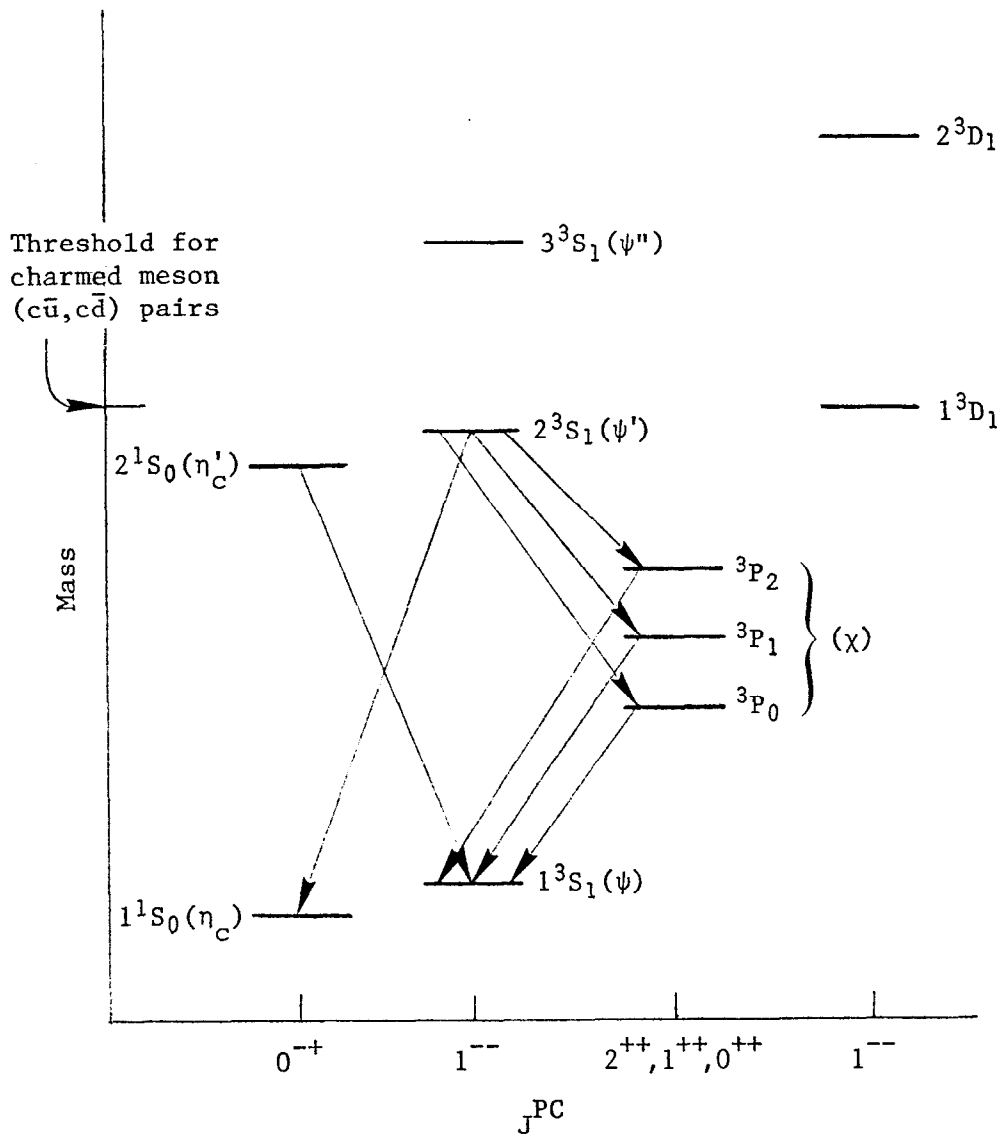


Fig. 24--The spectrum of charmonium ($c\bar{c}$).

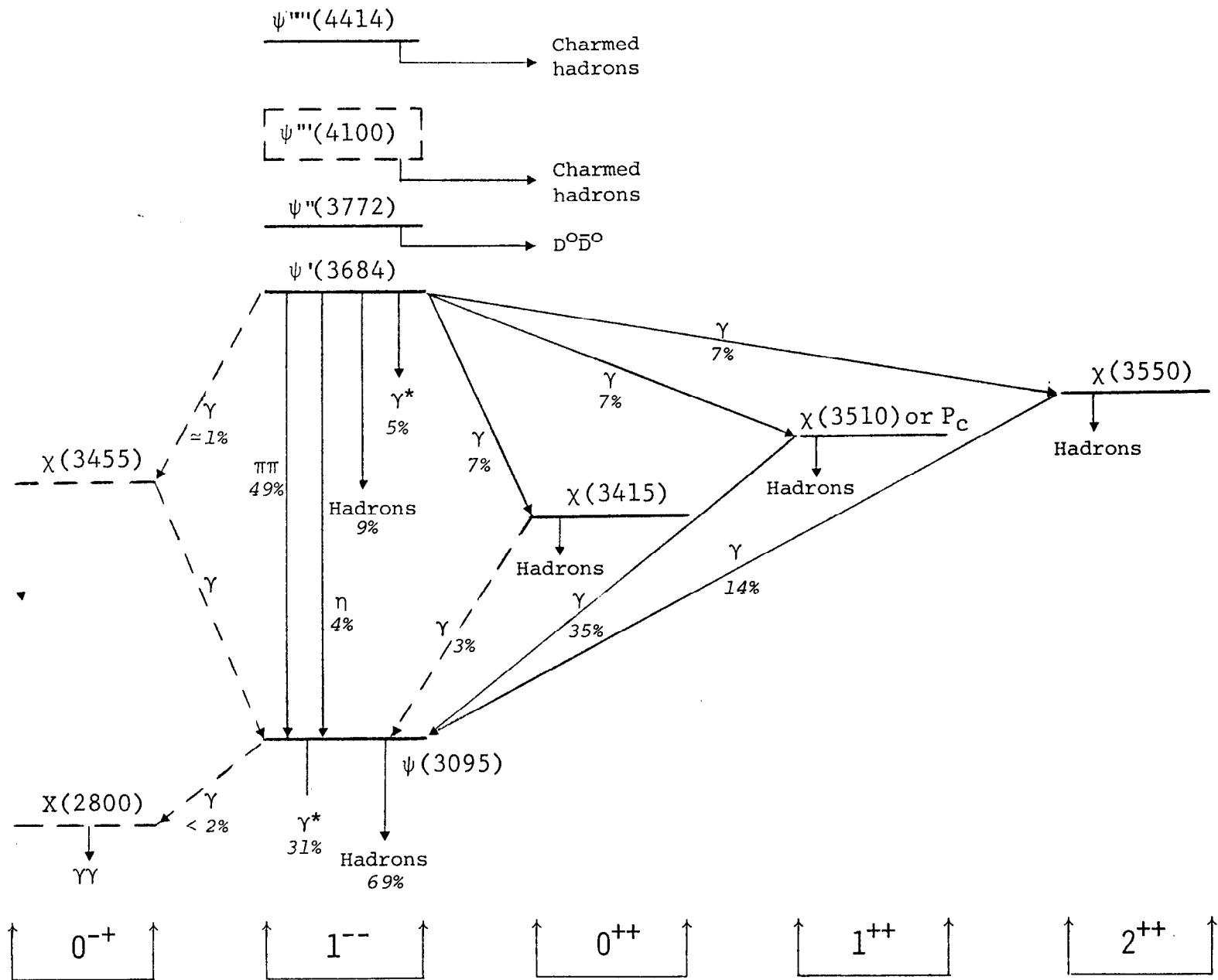


Fig. 25

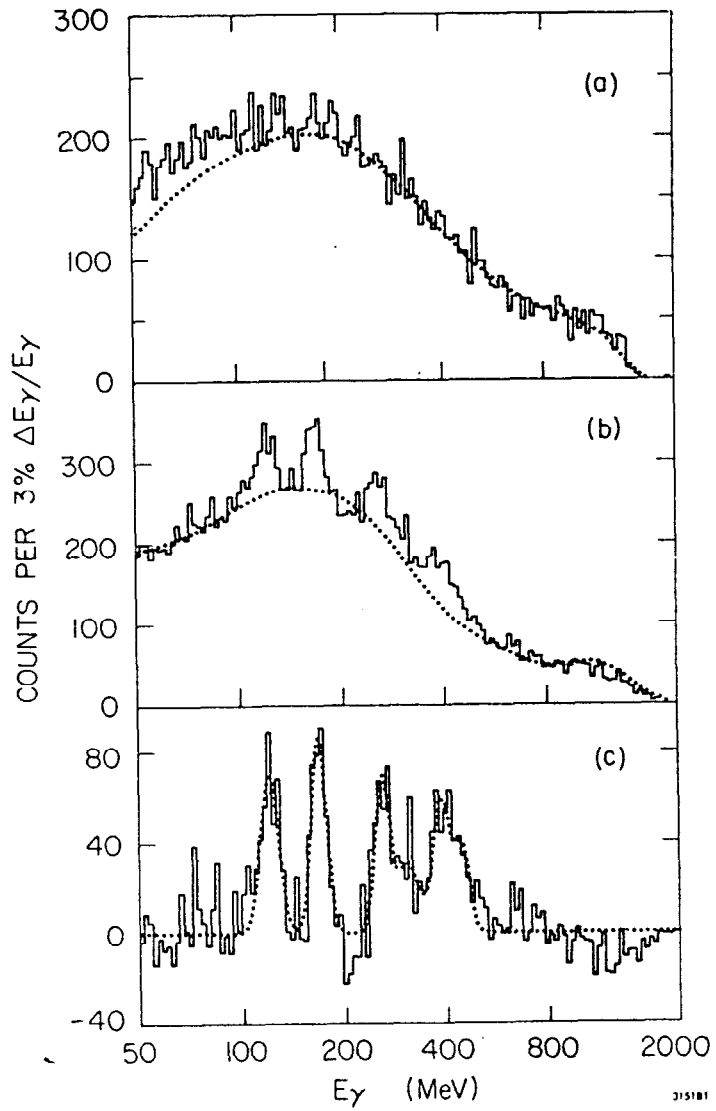


Fig. 26--The inclusive gamma-ray spectra for radiative decays of (a) $\psi(3095)$ and (b) $\psi'(3684)$. Part (c) shows the $\psi'(3684)$ results with the dotted curve in (b) set to zero in (c).

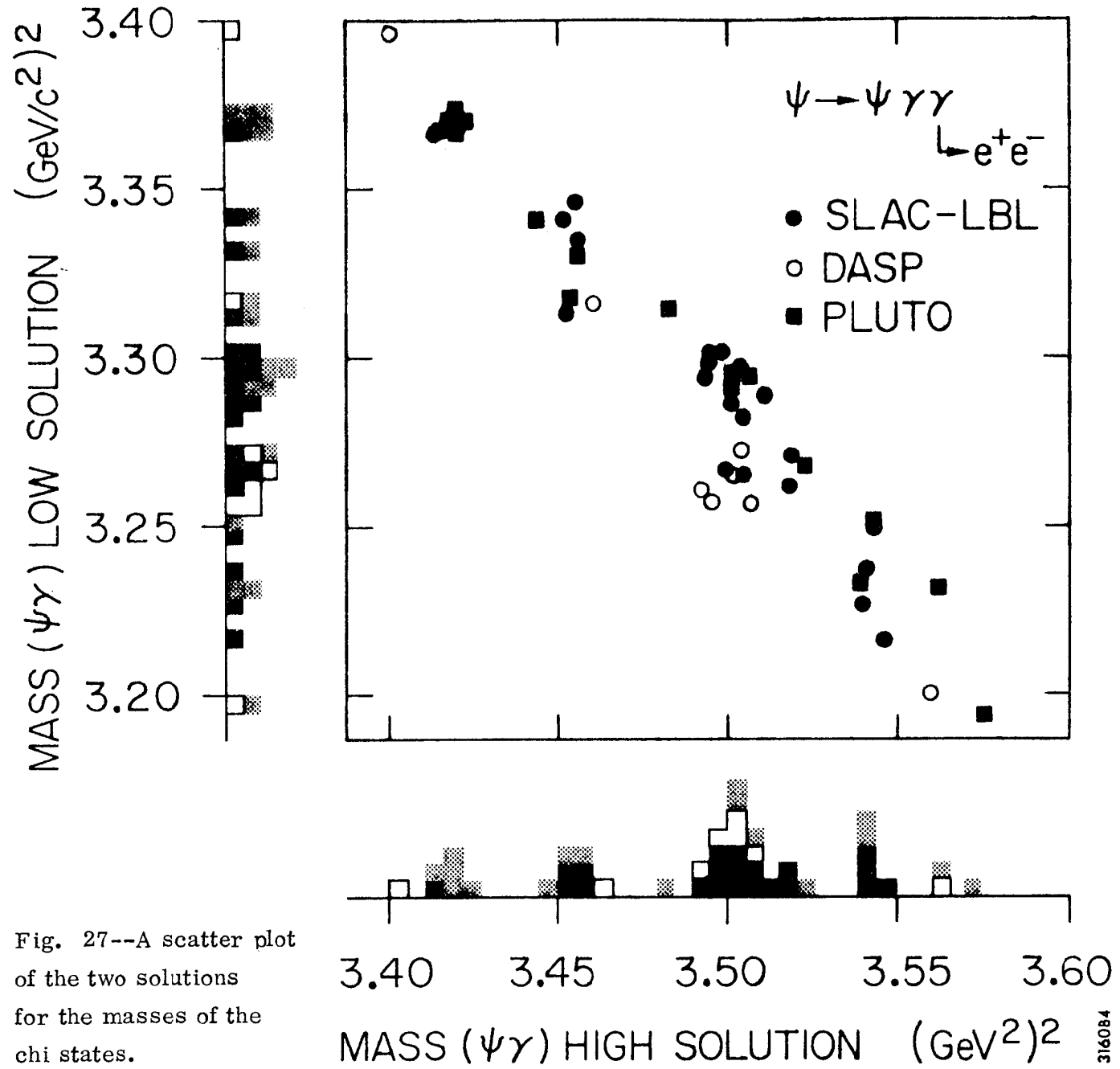


Fig. 27--A scatter plot of the two solutions for the masses of the chi states.

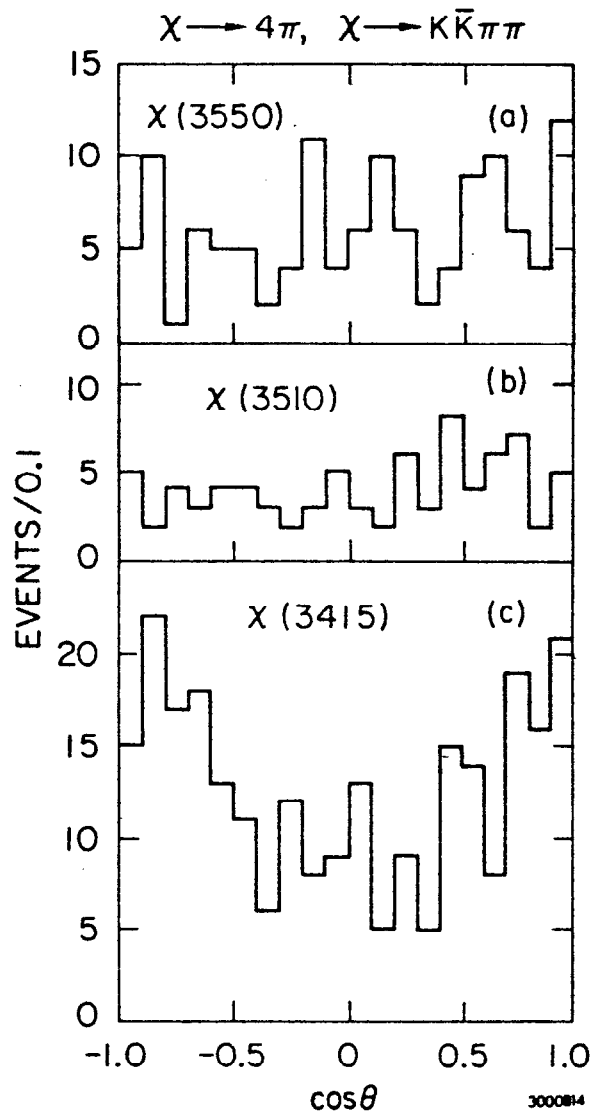


Fig. 28--Angular distribution of the photons from radiative decay of three chi states.

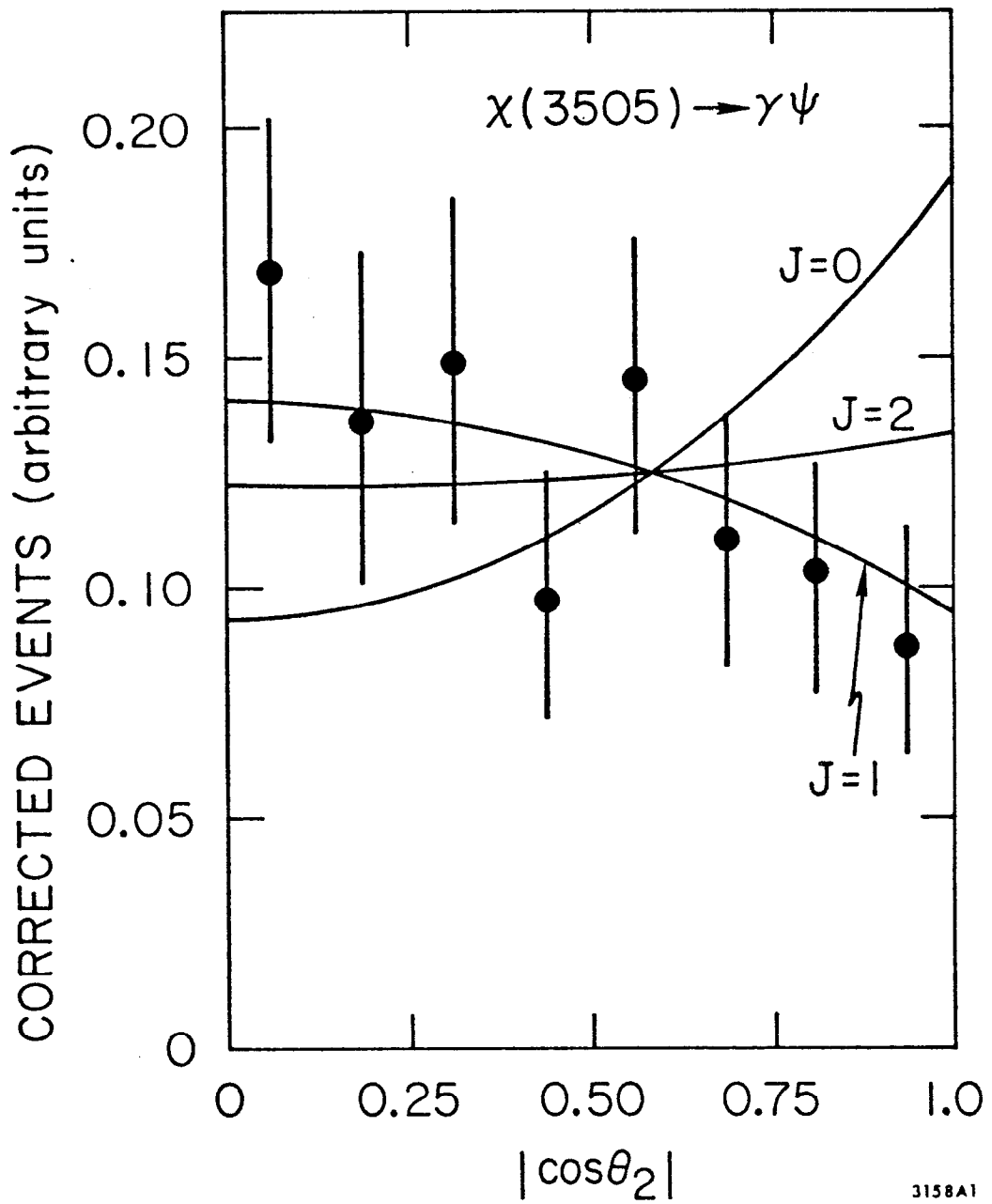


Fig. 29--Angular distribution of the photons emitted in the decay $\chi(3505) \rightarrow \gamma\psi$ in comparison with the predictions derived from spin assumptions $J = 0, 1, 2$.

State/ J^P	0^-	0^+	1^+	2^+
$\chi(3550)$	Excluded by $\chi \rightarrow \pi^+\pi^-$ or K^+K^- and by angular distribution in $\psi' \rightarrow \gamma\chi \rightarrow \gamma\text{hadrons}$	Excluded by angular distribution in $\psi \rightarrow \gamma\chi \rightarrow \gamma\text{hadrons}$	Excluded by $\chi \rightarrow \pi^+\pi^-$ or K^+K^-	PREFERRED
$\chi(3510)$	Excluded by angular distribution in $\psi \rightarrow \gamma\chi \rightarrow \gamma\gamma\psi$	Excluded by angular distribution in $\psi \rightarrow \gamma\chi \rightarrow \gamma\gamma\psi$	PREFERRED	
$\chi(3455)$	PREFERRED			
$\chi(3415)$	Excluded by $\chi \rightarrow \pi^+\pi^-$ or K^+K^-	PREFERRED	Excluded by $\chi \rightarrow \pi^+\pi^-$ or K^+K^-	

Fig. 30--Summary of the chi assignments.

$$m_u \approx 1/2 m_\rho = 0.39 \text{ GeV}$$

$$m_d \approx 1/2 m_\rho = 0.39 \text{ GeV}$$

$$m_s \approx 1/2 m_\phi = 0.51 \text{ GeV}$$

$$m_c \approx 1/2 m_\psi = 1.55 \text{ GeV}$$

Fig. 31--Estimated masses of the quarks, assuming that their binding energies are weak in the lightest vector mesons.

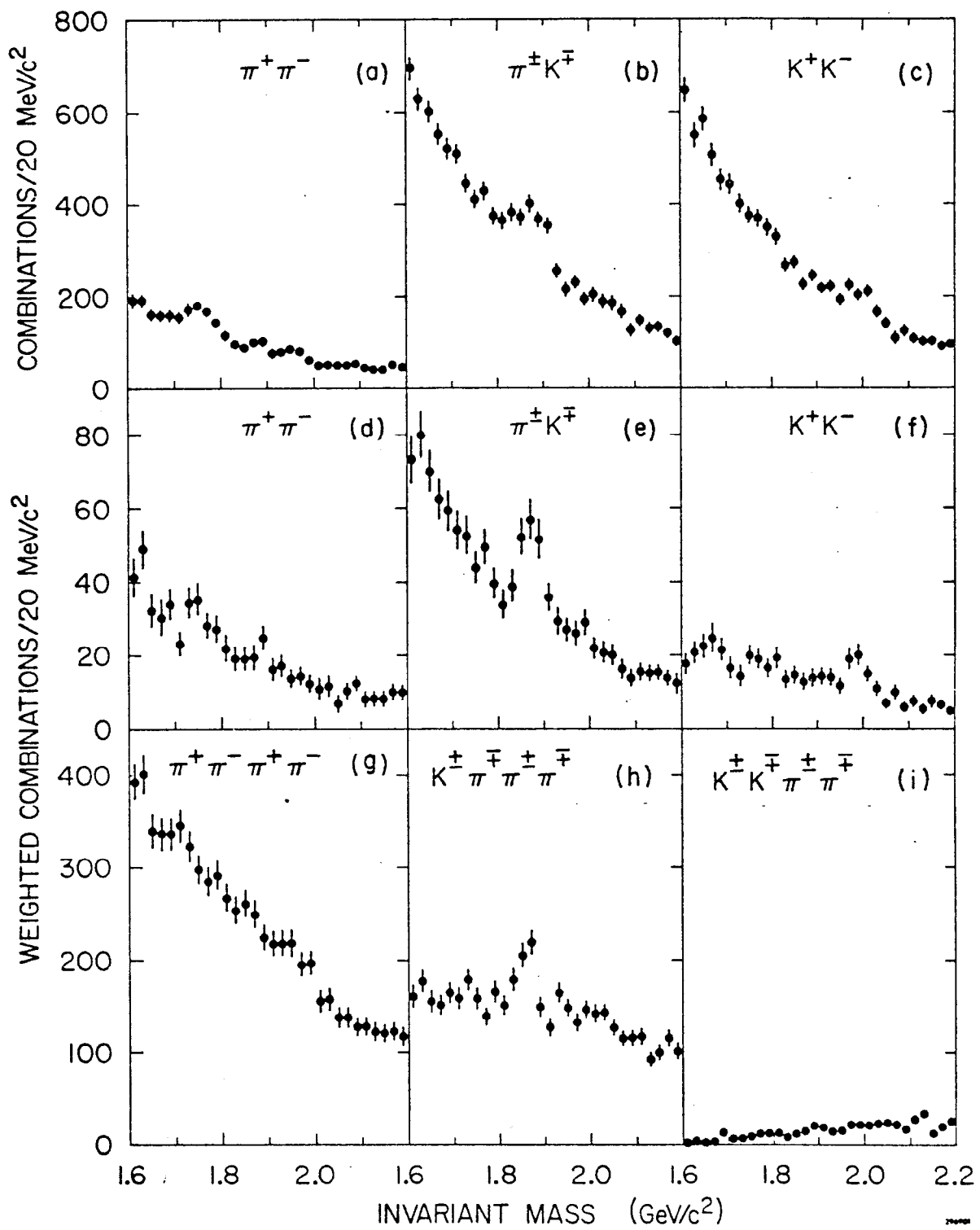


Fig. 32

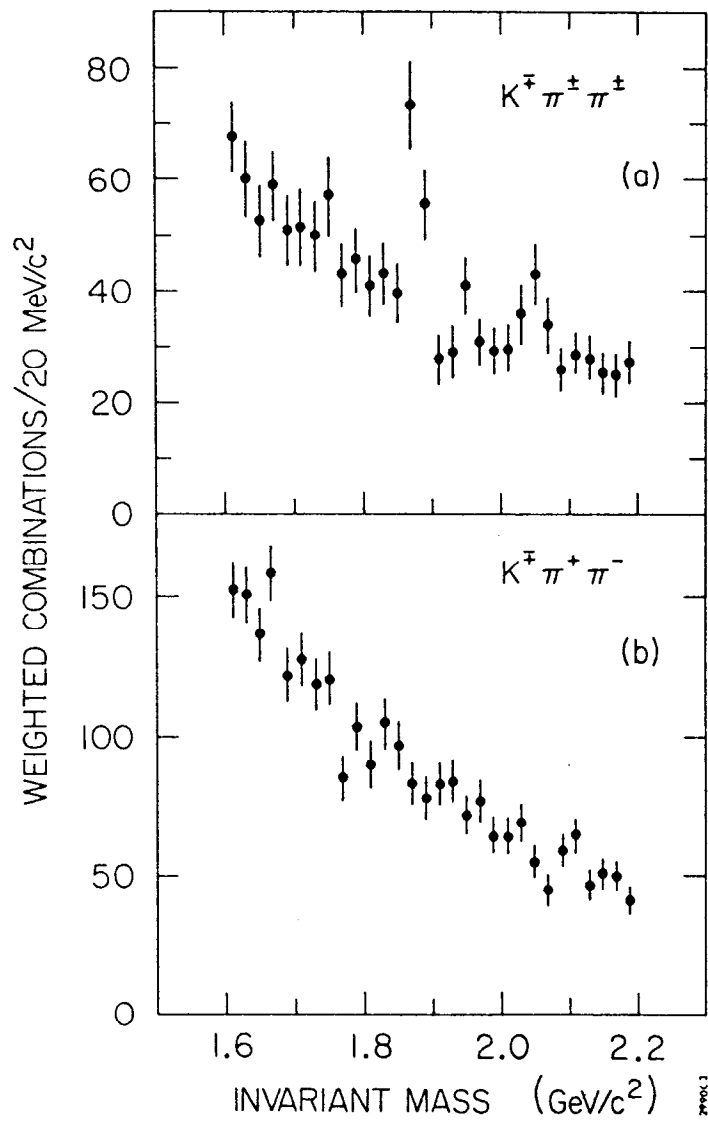


Fig. 33

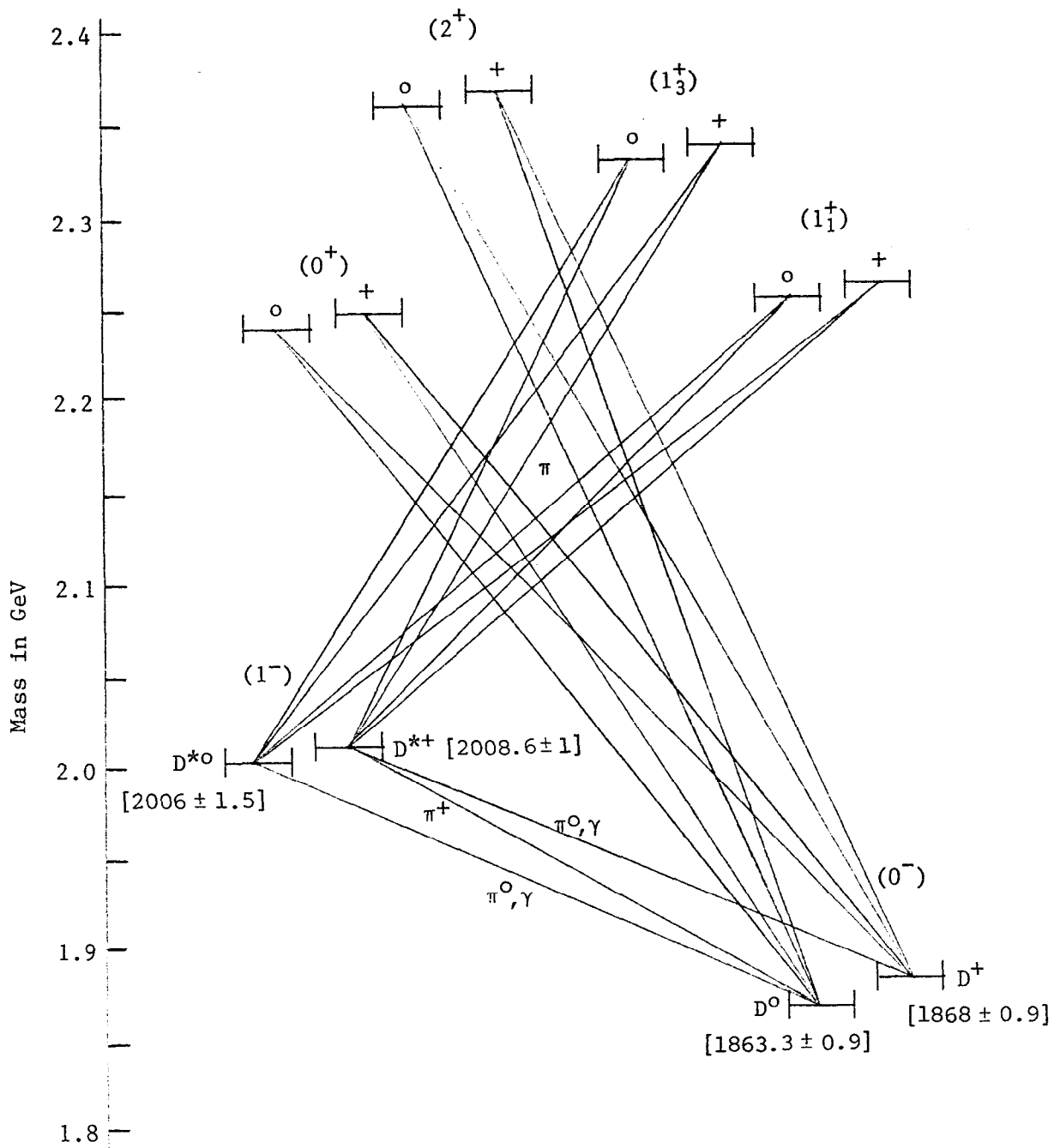


Fig. 34--The predicted spectrum of charmed D mesons ($c\bar{u}$ and $c\bar{d}$). The F mesons ($c\bar{s}$) are not shown here. The masses of the four low-lying states have been determined to the accuracies shown in the square brackets (mass in MeV).

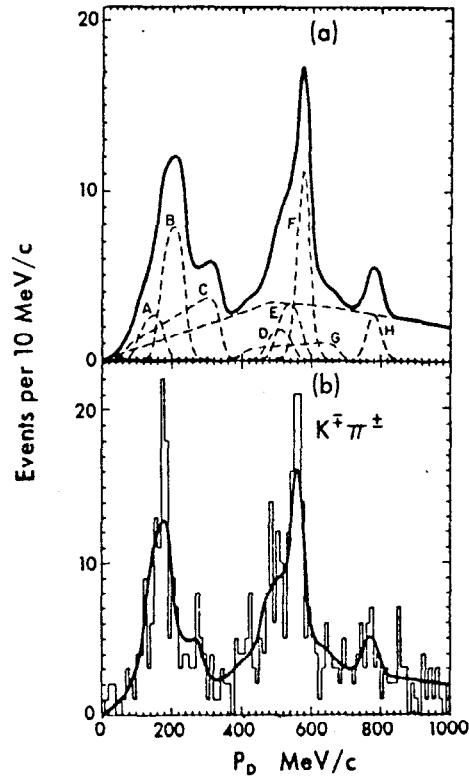


Fig. 35. (a) Illustrative example of the contributions to the expected D^0 momentum spectrum near threshold:

- | | |
|---|--|
| (A) $e^+e^- \rightarrow D^{*+}D^{*-}$, $D^{*+} \rightarrow \pi^+D^0$ | (E) $e^+e^- \rightarrow D^{*0}\bar{D}^0$, $D^{*0} \rightarrow \pi^0D^0$ |
| (B) $e^+e^- \rightarrow D^{*0}\bar{D}^{*0}$, $D^{*0} \rightarrow \pi^0D^0$ | (F) $e^+e^- \rightarrow \bar{D}^{*0}D^0$ Direct D^0 |
| (C) $e^+e^- \rightarrow D^{*0}\bar{D}^{*0}$, $D^{*0} \rightarrow \gamma D^0$ | (G) $e^+e^- \rightarrow D^{*0}\bar{D}^0$, $D^{*0} \rightarrow \gamma D^0$ |
| (D) $e^+e^- \rightarrow D^{*+}D^-$, $D^{*+} \rightarrow \pi^+D^0$ | (H) $e^+e^- \rightarrow D^0\bar{D}^0$ Direct D^0 |

The unlabeled dashed curve corresponds to the smoothed background of uncorrelated $K^-\pi^+$ combinations. (b) The observed $D^0 \rightarrow K^-\pi^+$ momentum spectrum at $E_{\text{cm}} = 4.028$ GeV. The solid curve is a typical fit to the data based on detailed estimates of contributing channels, masses and branching ratios.

	D		F
Charm	+1		+1
Isospin	1/2		0
Strangeness	0		+1
Quark Content	$c\bar{d}$	$c\bar{u}$	$c\bar{s}$
Pseudoscalar Name	D^+	D^0	F^+
Vector Name	D^{*+}	D^{*0}	F^{*+}

Fig. 36--Quark content and internal quantum numbers of the D and F singly charmed mesons.